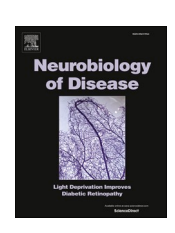
ELSEVIER

Contents lists available at ScienceDirect

Neurobiology of Disease

journal homepage: www.elsevier.com/locate/ynbdi



Early social deficits in TgF344-AD rats are accompanied by sex-specific parvalbumin-positive interneuron reduction and altered brain oscillations in the hippocampal CA2

Daniela Černotová ^{a,b}, Karolína Hrůzová ^{a,b}, Jan Touš ^{a,c}, Radek Janča ^c, Aleš Stuchlík ^a, David Levčík ^{a,*,1}, Jan Svoboda ^{a,1}

ARTICLE INFO

Keywords: Alzheimer's disease TgF344-AD Social memory CA2 Hippocampus Parvalbumin-positive interneurons

ABSTRACT

Social withdrawal and deficits in social cognition are hallmarks of Alzheimer's disease (AD). While early deficits in social behavior and memory have been documented in mouse AD models, they remain understudied in rat models. Early-stage AD is accompanied by dysfunction of parvalbumin-positive (PV+) interneurons, implicating their potential connection to early symptoms. In this study, we employed a 5-trial social memory task to investigate early deficits in social cognition in 6-month-old TgF344-AD male and female rats. We counted the number of PV+ interneurons and recorded local field potentials during social interactions in the hippocampal CA2 – a region critical for social information processing. Our results show decreased social interest and novelty preference in TgF344-AD male and female rats. However, reduced PV+ interneuron numbers were observed only in female rats and specific to the CA2 area. The electrophysiological recordings revealed reduced theta-gamma phase-amplitude coupling in the CA2 during direct social interactions. We conclude that deficits in social cognition accompany early-stage AD in TgF344-AD rats and are potentially linked to PV+ interneuron and brain oscillatory dysfunction in the CA2 region of the hippocampus.

1. Introduction

Social withdrawal and deficits in social cognition are key features of Alzheimer's disease (AD) (Amlerova et al., 2022; Flicker et al., 1990; Jost and Grossberg, 1996; Mazzi et al., 2020; Nelis et al., 2011; Savaskan et al., 2018). Evidence suggests that social isolation not only increases the risk of developing dementia (Livingston et al., 2017) but can also accelerate AD progression (Huang et al., 2015; Dong et al., 2004). These social changes can, however, also be an early manifestation of the disease itself. This is well-demonstrated in transgenic AD models, where early alterations in social behavior are observed and characterized as decreased social interest (Chaney et al., 2021; Kosel et al., 2019; Pietropaolo et al., 2012) or impaired social memory (Cheng et al., 2013; Deacon et al., 2009; Filali et al., 2011; Locci et al., 2021; Rey et al., 2022).

Social interactions represent a complex form of behavior, engaging

several brain structures critical for emotional and memory processing, including the prefrontal cortex, amygdala, and hippocampus (Ko, 2017). The coordination of these brain regions is mediated by inhibitory parvalbumin-positive (PV+) interneurons (Ognjanovski et al., 2017; Xia et al., 2017). Within the hippocampus, the inhibitory tone is enhanced particularly in the dorsal CA2 (dCA2), where PV+ interneurons dominate in the pyramidal layer and occur at higher densities than in other hippocampal regions (Botcher et al., 2014; Piskorowski and Chevaleyre, 2013). The dCA2 plays a crucial role in detecting social novelty, and its proper function is essential for social memory processing (Hitti and Siegelbaum, 2014; Stevenson and Caldwell, 2014).

Post-mortem analysis of the brains of elderly AD patients revealed a significantly reduced number of PV+ interneurons in the CA1, CA2, and dentate gyrus (Brady and Mufson, 1997). Fewer PV+ interneurons were also found in the dCA2 of 9- to 10-month-old Tg2576 mice with human APPswe mutation and progressive β -amyloid plaque accumulation,

a Laboratory of Neurophysiology of Memory, Institute of Physiology of the Czech Academy of Sciences, Videnska 1083, Prague 142 00, Czech Republic

^b Third Faculty of Medicine, Charles University, Ruska 87, Prague 100 00, Czech Republic

^c Faculty of Electrical Engineering, Czech Technical University in Prague, Technicka 2, Prague 160 00, Czech Republic

^{*} Corresponding author.

E-mail address: david.levcik@fgu.cas.cz (D. Levčík).

 $^{^{1}\,}$ These authors contributed equally.

starting at this age (Hsiao et al., 1996; Rey et al., 2022). These mice showed impaired social memory, but their sociability was unaffected (Rey et al., 2022). Distinct alterations in PV+ interneuronal proteome were recently described in 3-month-old 5xFAD mice with plaque deposits present from the 2nd month and linked to the severity of cognitive decline and neuropathology in AD patients (Oakley et al., 2006; Kumar et al., 2024). Nevertheless, evidence gathered in animal research suggests that PV+ interneurons might be affected sooner, even before amyloid plaque accumulation (Černotová et al., 2023). Not much is known about how the pathophysiology of dCA2 affects social behaviors and cognition in AD. The existing findings pose intriguing questions about potential disruptions in social cognition and pathophysiological changes in the hippocampal dCA2 in the early stages.

Most of the research mentioned earlier was performed in mice. Rat models of AD are sparse, even though they may be more suitable for examining behavioral changes and early pathology – they have complex social behaviors (Schweinfurth, 2020) and are physiologically and genetically closer to humans than mice (Do Carmo and Cuello, 2013). In this study, we aimed to investigate early social cognition deficits in the TgF344-AD rat model of AD. These transgenic rats exhibit β-amyloid plaque accumulation, tau pathology, and progressive cognitive decline (Cohen et al., 2013). We tested 6-month-old male and female rats, given that this age can be characterized as an early-plaque stage: the cognitive functions are still preserved, and β-amyloid merely starts accumulating in the hippocampus, including dCA2 (Cohen et al., 2013). We first performed the 5-trial social memory task, hypothesizing that the TgF344-AD (= AD) rats would demonstrate decreased social interest and novelty preference compared to wild-type (= WT) controls. Given the importance of the hippocampal dCA2 in social memory processing, we sought to elucidate early neurophysiological alterations in this area. Specifically, we used immunohistological methods to quantify PV+ interneurons and in vivo electrophysiology to measure local field potentials (LFPs) in dCA2 in behaving animals during social and non-social tasks. We further counted the PV+ interneurons in dCA1 and basolateral amygdala (BLA) to compare PV+ cell densities in other brain regions.

This study provides insights into early social cognition impairments

in TgF344-AD male and female rats and presents the first evidence for a sex-specific reduction in PV+ interneuron number and impaired social information processing in the hippocampal dCA2. Together, the results show that deficits in social cognition accompany early-stage AD in TgF344-AD rats, with potential links to PV+ interneuron dysfunction and impaired oscillatory coupling in the dCA2.

2. Materials and methods

2.1. Animals

Six-month-old wild-type Fisher 344 rats (WT group, N = 9 females and N=10 males) and TgF344-AD rats (AD group, N=12 females and N = 12 males) underwent the five-trial social memory task and the hidden food test. The brains of these rats were then used for immunohistological procedures, with four additional rats (two males and two females) for RGS14 immunostaining of dCA2. Another cohort (WT (N = 20) and AD (N = 14) male rats) was used for in vivo electrophysiological recordings during resting state and the five-trial social and object memory tasks (Fig. 1A). The rats, obtained initially from RRRC, Missouri, were bred at the Animal Facility of the Institute of Physiology CAS and housed in pairs in a room with controlled conditions (22 °C, 50-60 % humidity, 12 h light/dark cycle) and dimmed light (<50 lx) to avoid retinal degeneration (Semple-Rowland and Dawson, 1987). The TgF344-AD colony was maintained by mating transgenic hemizygotes with their wild-type counterparts, resulting in an approximately equal distribution of TgF344-AD and wild-type siblings. At the age of three weeks, their genotypes were determined through a PCR analysis from a small piece of tissue, which had been collected from the tip of the tail under isoflurane anesthesia. All animal experiments complied with ARRIVE (Animal Research: Reporting of In Vivo Experiments) guidelines. All animal treatments were approved by the Local Animal Care Committee (51-2022-P) and complied with the Animal Protection Code of the Czech Republic and the European Community Council directive (2010/63/EC). Maximum efforts were made to minimize the suffering of animals.

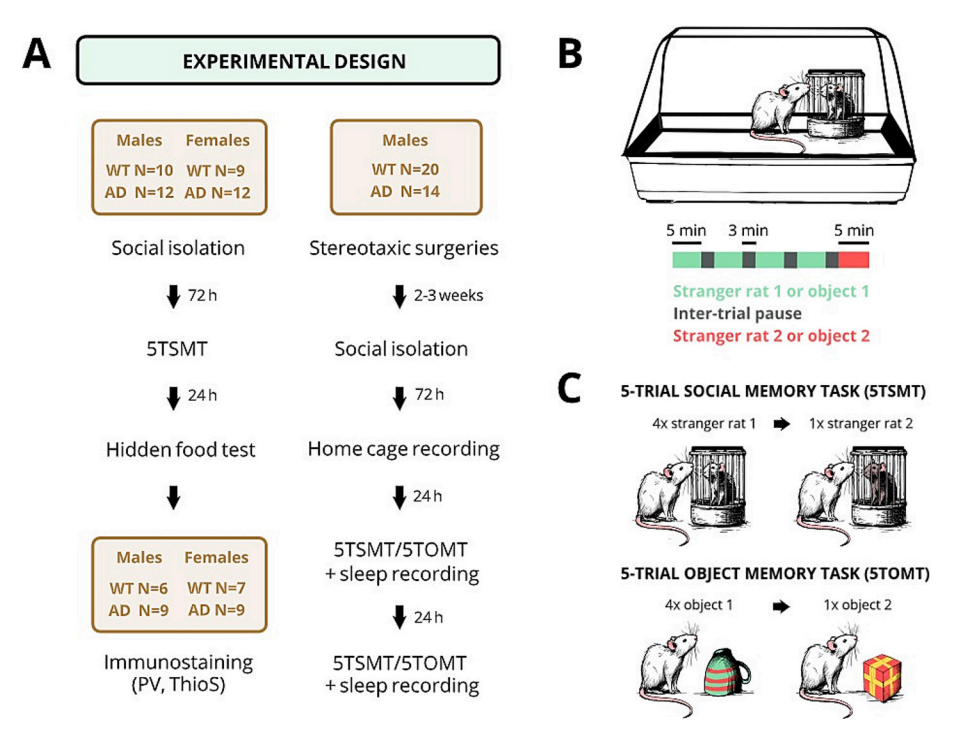


Fig. 1. Schematic representation of the experimental design (A) and experimental protocol for the five-trial social and object memory tasks (B–C). A subject rat was introduced to the first stranger rat or unknown object in their home cage for four consecutive five-minute trials. Then, the second stranger rat or object was introduced for another 5 min. The inter-trial interval lasted 3 min.

2.2. Five-trial social memory task (5TSMT)

The 5TSMT evaluates the ability to recognize familiar conspecifics. Briefly, a stranger rat is presented to the subject rat for four consecutive five-minute trials (t_1-t_4) (Fig. 1C). Then, a novel stranger rat is presented for 5 min in the fifth trial (t_5) . Repeated exposure to the same stranger rat should decrease the social interest of the subject rat (habituation). In contrast, subsequent exposure to another stranger rat should arouse natural interest due to the novelty effect (Thor and Holloway, 1982). Three-minute intervals between trials were used.

All rats underwent two days of habituation to the experimenter and experimental room. Stranger rats were additionally habituated to a small cage with a circular platform (12 cm in diameter) and metal bars (15 cm in height, 1 cm between bars) for three days (1–2 times/day with increasing intervals of 5-20 min). Stranger rats were always the same sex as the subject rats, came from a different litter, and were younger (two to three months) to decrease potential adult male aggressive behavior (Thor and Holloway, 1982). On the last day of habituation, all rats were placed into separate home cages ($42 \times 28 \times 22$ cm) and kept in isolated conditions for 72 h to increase social motivation (Toyoshima and Yamada, 2023). Before initiating the behavioral task, subject rats were habituated to the experimental room for at least 30 min and then to the empty small cage for 5 min. The experiment was performed in the rats' home cage. The small cage with stranger rats was put on one side of the home cage, with free space around the cage so the subject rats could move around and explore (Fig. 1B). One top-view and one front-view camera were used for the recording of experiments (30 FPS, 1920 \times 1080 resolution). All experiments were performed between 8:30 am and 2:00 pm in a room with dimmed light (10 lx).

2.3. Five-trial object memory task (5TOMT)

For the electrophysiological experiments, we also performed a non-social control test to record the activity of the hippocampal dCA2 region while processing non-social stimuli. We followed the 5TSMT design in this task but replaced rats with objects. The first object (trials 1–4) was a green cup (9 cm diameter, 8 cm height) with red horizontal stripes and oregano odor. The second object (trial 5) was a red box (6 \times 6 \times 6 cm) with yellow vertical stripes and parsley odor (Fig. 1C). Each trial again lasted 5 min with three-minute inter-trial intervals.

2.4. Hidden food test

The hidden food test was performed to confirm intact olfaction, which is crucial for social interactions and may be impaired in early-stage AD (Roberts et al., 2016). For this experiment, rats were kept on a restricted diet (85–90 % of standard weight, no food 24 h before the test). On the first two days, two cereal cocoa balls (BONAVITA, Czech Republic) were placed on each side of a home cage (42 \times 28 \times 22 cm) under the bedding to habituate the rat to the cocoa balls. On the third day, each rat was placed in a new cage with a 4 cm high bedding layer, where two cocoa balls were hidden 1 cm under the bedding at either the left or right side of the cage. The rats were then video-recorded with a front-view camera for 15 min. The test was finished after the rat had found the reward or after 15 min had elapsed.

2.5. Stereotaxic surgeries

For the electrophysiological experiment, male WT (N = 20) and AD (N = 14) rats were implanted with recording electrodes in dCA2. A custom-made implant consisted of two bundles of four nickel-chrome electrodes (0.0762 mm diameter, 0.07 mm length; CFW, USA) placed in 22 gauge cannulas (inner diameter 0.65 mm). The endings of the electrode bundles were cut diagonally to cover the shape of the dCA2 region. Cannulas were attached to a 3D-printed plate, and electrodes were attached to a connector (Mill-Max, USA) using gold-plated pins

(Neuralynx, USA). One ground and one reference screw was attached to the implant. The electrodes served to record hippocampal local field potentials (LFPs) in both hemispheres. Two additional silver wires (0.254 mm diameter; A-M Systems, USA) with unisolated loop-twisted endings were inserted bilaterally under the skin near the temporalis muscles for recording muscle activity.

Rats were treated with antibiotics dissolved in drinking water (enrofloxacin, 100 mg/ml) one week before the surgeries. The rats were induced to an esthesia with 5 % isoflurane and maintained at 1.2 % to 2.5% during surgeries. The cannulas with electrodes were inserted into the brain through small drilled holes in the skull at coordinates corresponding to the hippocampal dCA2 region (AP = -3.5 mm, ML $= \pm 3.7$ mm, DV = 3.5-3.6 mm from bregma, according to the brain atlas; Paxinos and Watson, 2007). One ground and reference screw was placed above the cerebellum. Two anchoring screws were additionally placed anteriorly to the electrodes. The implant was then attached to the screws and skull with methacrylate resin. The incision was sutured and treated with mesocain (10 mg/ml). Shortly before awakening, rats were treated subcutaneously with 10 % carprofen (50 mg/kg). Rats with electrophysiological implants were kept in groups of two to three in larger plastic cages (55 \times 35 \times 27 cm) to decrease the risk of implant damage. Antibiotics (enrofloxacin, 100 mg/l) and analgesics (ibuprofen, 100 mg/ 1) were administered in drinking water for five days after the surgery. Rats were monitored daily for health status and left for complete recovery for at least two weeks before the experiments.

2.6. Electrophysiological experiments

As only male rats of both genotypes habituated to the stranger rat in the 5TSMT (Fig. 3), we chose to exclude females from the electrophysiological experiments. We recorded LFPs in the dCA2 during rats' resting state (= quietly awake, resting, or in a relaxed state without active exploration), the 5TSMT (social variant), and 5TOMT (object variant). Before the start of electrophysiological recordings, rats were habituated to the headstage connection and free movement with the connected headstage cable for five days. Then, three days of experiments followed. On the first day, the rats were recorded for 2 h in their home cage (55 \times 35 \times 27 cm). On the second day, the rats were recorded during the 5TSMT, and on the third day, they were recorded during the 5TOMT. This order was valid for half of the transgenic and control rats tested. The other half of the rats were tested in the reverse order (object variant on day 2, social variant on day 3). At the end of the task, rats were always left in their home cage, and the resting state LFP activity was recorded for an additional 2 h. Initially, we aimed to analyze the sharpwave ripple incidence and characteristics during the two-hour sleep recordings that followed both behavioral tasks. Unfortunately, we observed significant signal distortion in the 150-250 Hz frequency band, critical for sharp-wave ripple detection. Therefore, we omitted post-task sleep recordings from the analysis. All rats were tested at 5.5 to 7 months of age.

Data from all recording electrodes were amplified $(1000\times)$ using Lynx-8 amplifiers (Neuralynx, USA). The signal was band-pass filtered at 1–475 Hz at a sampling rate of 2000 Hz. A Micro 1401-3 system (CED, UK) recorded the neural activity.

2.7. Immunohistochemistry

Rats were perfused transcardially with 0.1 M PB, then 4 % PFA. The brains were carefully removed and post-fixed in 4 % PFA overnight, then put in 30 % sucrose + 0.1 M PB solution until sunk. Afterward, they were deep-frozen in dry ice. The brains were cut into 40 μm coronal slices using Leica cryostat and stored at $-20~^{\circ}\text{C}$ for further processing.

2.7.1. PV+ interneuron immunostaining

Brains of unimplanted rats that underwent the 5TSMT and the hidden food task were collected and used for immunostaining the

interneurons containing PV. One experimental batch of rats was not perfused after the behavioral testing, and one AD female brain was excluded from the count due to damage. Therefore, the final number of collected and stained brains was six WT males, nine AD males, seven WT females, and seven AD females. Diaminobenzidine tetrahydrochloride (DAB) staining was used to visualize PV+ interneurons. Every sixth slice was collected and thoroughly washed as free-floating sections in $1\times$ PBS. The slices were incubated in 10 % methanol, 1 % H_2O_2 , and $1 \times PBS$ solution for 30 min, followed by a blocking serum (5 % bovine serum +0.3 % Triton in $1\times$ PBS) for another 30 min. Then, the slices were incubated overnight in a fresh blocking serum with anti-PV rabbit antibody (1:1000, #ab11427, Abcam) on a shaker at 7 °C. On the second day, the slices were washed in $1 \times PBS$ and incubated in biotinylated anti-rabbit antibody (1:500, #SAB4600006, Sigma Aldrich) for $2\,\mathrm{h}$, then with ABC-HRP solution (9 μl of each component / 1 ml PBS, #PK-6100, Vector Laboratories) for 1 h. The staining was finalized with 4-6 min long incubation in DAB solution (20 mg DAB (#D5905, Sigma Aldrich) dissolved in 50 ml $1\times$ PBS with 15 μ l 30 % H_2O_2 , added right before the staining). The slices were washed with tap water, then $1 \times PBS$, and mounted on gelatin-coated slides. After drying, the slices were soaked in Neo-Clear and coverslipped using Neo-Mount.

2.7.2. RGS14 staining

Every sixth slice was collected and washed as free-floating sections in $1\times$ PBS. Antigen retrieval was performed (30 min incubation in 10 mM sodium citrate, pH 8.5, 80 °C), and slices were left to cool at room temperature. The slices were then incubated in a blocking serum (5 % bovine serum + 0.3 % Triton in $1\times$ PBS) for 1 h, followed by overnight incubation with anti-RGS14 mouse antibody (1:400, #75–170, Neuro-Mab) on a shaker at 7 °C. On the second day, the slices were washed in $1\times$ PBS and incubated in the secondary antibody (1:500, #A32742, Invitrogen) for 2 h. The slices were washed with $1\times$ PBS, mounted on gelatin-coated slides, and coverslipped using VectaShield.

2.7.3. Thioflavin S (ThioS) staining

Slices were mounted and dried on gelatinized slides. Then, they were washed in 70 % EtOH (3 min), 50 % EtOH (5 min), 1 % Thioflavin S dissolved in 50 % EtOH (11 min, #T1892, Sigma-Aldrich), 50 % EtOH (3 min), 70 % EtOH (5 min), ddH2O (wash), 0.1 M PB (10 min), and coverslipped using VectaShield.

2.7.4. Electrode placement verification

Every fourth slice was collected and processed with standard Nissl staining to verify the placement of recording electrodes. The exact location was verified according to the rat brain atlas (Paxinos and Watson, 2007).

2.8. Data analysis

Statistical analyses of data from behavioral experiments and all graphs were made in GraphPad Prism 10.4.0. Electrophysiological data analyses were conducted in Matlab (R2022b, Mathworks) using custom-made scripts. The significance level was set at p < 0.05. Unless otherwise stated, graph data are represented as the mean \pm standard error (SEM).

2.8.1. Behavioral data analysis

The total sniffing duration of the stranger rats or objects was counted during the five-minute trials. Subject rats were tagged as "sniffing" when either poking their nose between bars in the cage with a stranger rat, sniffing at the stranger rat's tail, or sniffing at the lower half of the cage. The behavior was not counted when the experimental rat explored the cage's upper lid or cage bars. Accordingly, "sniffing" was counted when closely exploring the objects in the 5TOMT. The sniffing duration was measured from recordings taken on a front-view camera. If the experimental rat was not seen on the front-view camera, the analysis continued on the top-view camera. Behavioral data were analyzed in

BORIS v. 7.10.5 (Friard and Gamba, 2016). The person analyzing behaviors was blinded to the experimental group.

A robust regression and outlier removal test was performed in behavioral 5TSMT and 5TOMT tasks to identify outliers ($Q=1\,$ %). When a rat was identified as an outlier in more than 2 trials or did not interact with stranger rats or objects at all, it was excluded (outliers: 1 female AD rat in the 5TSMT; non-interacting rats in the electrophysiological cohort: one WT rat in the 5TSMT, two AD and two WT rats in the 5TOMT). The male and female groups were analyzed separately. Parametric assumptions of data were tested with the Shapiro-Wilk test for normality of residuals. Data sets that were not normally distributed (all 5TSMT and 5TOMT data) were first logarithmically transformed using the ln(y + 10) formula. A two-way ANOVA (group \times trial) was used to analyze the 5TSMT and 5TOMT, followed by Sidak's multiple comparisons test if significant. All two-way ANOVA results are reported in Supp. Table 5, post-hoc tests are reported in Supp. Tables 1 and 2. The data from the hidden food test were analyzed using the Mann-Whitney U test.

2.8.2. Immunohistochemical data analysis

ImageJ (v. 1.54f) was used to measure the brain areas, count PV+ interneurons, and evaluate the β -amyloid plaque load. The hippocampal dCA2 was selected based on the superimposition of RGS14 immunostaining (Fig. 5B). For dCA1, a region of interest was chosen proximally from the hippocampal apex. The counting included all hippocampal layers from -2.8 to -4.08 mm AP from bregma and was performed manually by an experimenter. The experimenter counting the cells was blinded to the experimental groups. The basolateral amygdala (BLA) was defined according to the atlas (Paxinos and Watson, 2007), and the PV+ interneurons were counted at the same parameter settings using Yen thresholding and custom-made ImageJ macro. Six images per rat were analyzed for each structure (dCA2, CA1, and BLA). Cell density was calculated by dividing the total cell count by the counted area (PV+ cells / mm³). The β-amyloid plaque load was quantified as a % fluorescent area in the whole dorsal hippocampus and the dCA2, using the superimposition of RGS14 immunostaining (Fig. 7D). The % fluorescent area was counted at the same parameter settings using thresholding and custom-made ImageJ macro. The PV+ cell counts and differences in the β-amyloid plaque load between groups were analyzed using the unpaired t-test or the Mann-Whitney U test, depending on the normality of the data. The one-sample Wilcoxon test was used to analyze the β -amyloid plaque load in WT and AD groups, specifically testing whether the plaque load significantly differed from zero.

2.8.3. Electrophysiological data analysis

For each animal that underwent the electrophysiological experiments, we chose the brain hemisphere with more accurate electrode placement in the dCA2 pyramidal layer and one electrode within this hemisphere with the best signal quality (minimal noise and recording artifacts) for subsequent data analysis. Nine WT and five AD rats were excluded from the study due to incorrect electrode placement, and three additional rats from the WT group were excluded for hummed electrophysiological signals. One rat from the WT group and one from the AD group were not recorded during the 5TSMT or 5TOMT due to technical issues, and, therefore, they were not included in the electrophysiological data analysis. In total, nine rats from the AD group and eight from the WT group were included in the analysis of LFPs. We analyzed data from one hemisphere for each rat, and it was balanced for side and genotype (WT: five left, three right, AD: four left, five right). The location of the electrodes used to analyze the electrophysiological data obtained from the individual included rats is illustrated in Fig. 2.

We calculated the power spectral density (PSD) to explore the neural dynamics and estimated theta-gamma phase-amplitude coupling (PAC) to compare the information processing between the WT and AD rats. We analyzed both parameters during the resting state (day $1-2\ h$ in the home cage) and interactions with the stranger rats (5TSMT) or objects (5TOMT). Such interactions had to be at least 7 s long to be included in

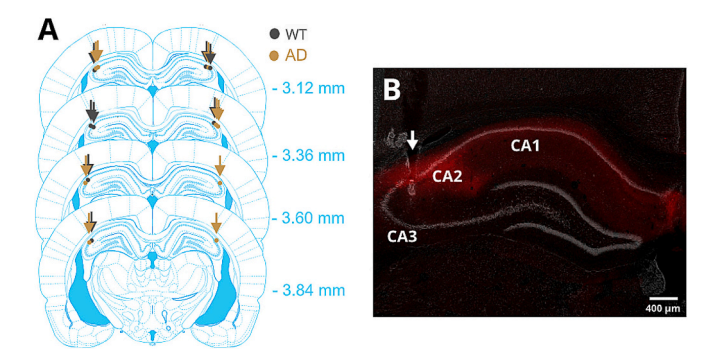


Fig. 2. Placement of electrode tips in the hippocampal dCA2 of rats included in the analysis (A) and a representative image of electrode placement in the dCA2, visualized by RGS14 staining (B). (A) Each dot represents one rat; black for WT (N=8), brown for AD (N=9). The AP coordinates of each coronal slice are written in blue. (B) The white arrow highlights the electrode position. Adapted from Paxinos and Watson (2007). (For interpretation of the references to colour in this figure legend, the reader is referred to the web version of this article.)

the analysis. We evaluated the seven-second periods as sufficient to estimate the cross-frequency PAC reliably. When multiple interactions occurred during a single session, we calculated the parameters for individual intervals, and the weighted arithmetic means for all intervals.

We pre-processed the neural data for all analyses and used a biquad filter to filter the 50 Hz component (power line noise) and its higher harmonic frequencies. The following steps were used to calculate the average PSD in each frequency band (delta: 1–4 Hz, theta: 4–10 Hz, alpha: 10–14 Hz, beta: 14–30 Hz, low gamma: 30–55 Hz and high gamma: 55–100 Hz). The LFP signal was divided into 50 % overlapping segments. An absolute Fourier spectrum was calculated for each segment and then averaged to estimate the PSD. The individual segments were multiplied by the Hanning window while estimating the PSD. Finally, the average PSD for the given frequency bands was calculated as the mean in these specific frequency bands.

To estimate cross-frequency interaction by PAC, we adopted the modulation index (MI) parametrization from Tort (Tort et al., 2008). The LFP signal was firstly band-pass filtered into the given frequency bands (theta, low gamma, high gamma) by a 20-order Butterworth bandpass filter. Analytical signals were obtained using the Hilbert transform — specifically, the instantaneous phase angle (for the lower frequency band) and instantaneous amplitude (for the higher band). To calculate the MI, all possible phases from -180° to 180° are first divided into 18 bins (20° step), and the corresponding average instantaneous amplitude was computed for each bin. The obtained phase-amplitude distribution (histogram) was normalized, and the Shannon entropy was calculated. PAC is defined as a distribution that deviates significantly from a uniform distribution, which was measured by the Kullback-Leibler distance. Finally, MI represents the ratio between the Kullback-Leibler distance to a uniform distribution.

We calculated PAC by the MI separately between theta and low gamma activity (4–10 Hz and 30–55 Hz) and between theta and high gamma (4–10 Hz and 55–100 Hz) activity. Parametric assumptions of MI descriptors were again tested with the Shapiro-Wilk test for normality of residuals and Spearman's test for heteroscedasticity. As most of the electrophysiological data did not meet the criteria for normal distribution, we compared them using the Mann-Whitney $\it U$ test.

3. Results

3.1. 5TSMT

In female rats, ANOVA results showed significant effects of trial (p < 0.0001), group (p = 0.02), and interaction (p = 0.0438). Post-hoc tests revealed a significantly lower investigation of the AD female group than

the WT female group in the first (p = 0.007) and fifth (p = 0.0055) trials. Moreover, WT females habituated to the first stranger rat (compared to t1: $p_{t2}>0.41,\,p_{t3}=0.0026,\,p_{t4}=0.0087)$ and spent significantly more time sniffing the second stranger rat ($p_{t4/5}=0.0054)$. Compared to WT females, AD females had reduced social interest, and therefore, no habituation was observed (compared to t1: $p_{t2}>0.96,\,p_{t3}>0.99,\,p_{t4}>0.20)$. Furthermore, AD females did not increase their interest in the second stranger rat ($p_{t4/5}>0.18$) (Fig. 3A).

In male rats, significant trial effect (p < 0.0001), a trend towards significant group (p = 0.0553) and significant interaction (p = 0.0362) effects were observed. Post-hoc tests revealed a significantly lower investigation of the AD male group compared to the WT male group in the first (p = 0.0124), second (p = 0.0189), and fifth (p = 0.0058) trials. When comparing the sniffing duration in the first trial to other trials, significant differences were found in both WT (pt2 = 0.041, pt3 < 0.0001, pt4 < 0.0001) and AD (pt2 = 0.024, pt3 = 0.0028, pt4 = 0.001) males, confirming habituation to the first stranger rat in both groups. However, only WT males increased their interest in the second stranger rat in the fifth trial (WT: pt4/t5 < 0.0001, AD: pt4/t5 = 0.63) (Fig. 3B). All post-hoc results are shown in Supp. Table 1.

3.2. Hidden food test

To exclude the olfactory impairment in AD rats, we evaluated if the rats could find hidden food equally to WT rats. One experimental batch was not used for this experiment. Thus, the number of tested rats was nine WT males, eleven AD males, eight WT females, and ten AD females. An unpaired t-test failed to reveal a significant difference between genotypes in females (p = 0.5138) or males (p = 0.669) (Fig. 4), confirming the rats could find hidden food equally.

3.3. PV+ interneuron count

We counted the PV+ interneurons in the dCA2 to investigate if the decrease in social interest and social memory impairment can be reflected in a differing number of these interneurons. The unpaired t-test showed that WT and AD male groups had a similar number of PV+ interneurons in the dCA2 (p = 0.5477), while AD females had fewer PV+ interneurons in the dCA2, compared to WT females (p = 0.0142) (Fig. 5A). To probe for the exclusivity of observed impairment, we counted the PV+ interneurons in dCA1 and BLA. There was no significant difference in the dCA1 between WT and AD females (p = 0.8746) nor WT and AD males (p = 0.8354) (Fig. 5C). Similarly, the number of PV+ interneurons did not differ in the BLA between WT and AD females (p = 0.3571) nor WT and AD males (p = 0.9076) (Fig. 6). This suggests that the impairment of PV+ interneurons is specific to the dCA2.

3.4. Amyloid plaque count

We counted the % fluorescent area in the hippocampus and the dCA2 to confirm the amyloid pathology and evaluate potential differences between sexes. Statistical results confirmed amyloid pathology with an approximate mean of 0.24 % (females) and 0.55 % (males) in the dCA2 (Fig. 7A) and 0.045 % in the whole hippocampus (both sexes) (Fig. 7C). In addition, no statistical difference was confirmed between AD females and males in the dCA2 (p = 0.536) (Fig. 7B).

3.5. Resting state neural activity

As only male rats of both genotypes showed habituation across the separate trials in previously performed 5TSMT (Fig. 3), we chose to exclude females from the electrophysiological experiments. We compared the PSD of individual frequency bands between WT and AD rats during the two-hour homecage recordings (day 1) to assess the effect of genotype on the dynamics of the resting state neural activity. No statistically significant differences were found using the Mann-Whitney

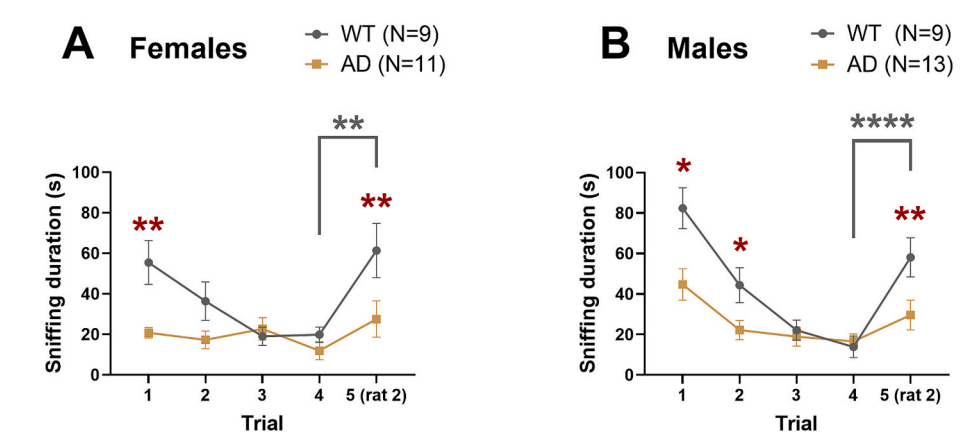


Fig. 3. Sniffing duration of stranger rats in the 5TSMT. Female rats showed significant trial, group, and interaction effects (A), while males demonstrated significant trial and interaction effects (B). Post-hoc analysis revealed reduced sniffing duration in AD groups compared to WT groups during trials 1 and 5 in both sexes, with males also showing a decrease in trial 2. All groups except AD females exhibited decreasing sniffing duration across trials 1–4, indicating normal habituation to the first stranger rat (detailed post-hoc results for trials are provided in the text and Supp. Table 1). When comparing sniffing durations between trials 4 and 5 (first vs. second stranger rat), both WT females and WT males spent significantly more time investigating the second stranger rat in trial 5, confirming a preference for social novelty. In contrast, AD rats showed no significant preference. Significant differences between WT and AD groups are indicated by red asterisks, while significant differences between trials 4 and 5 within WT groups are marked by grey asterisks. * indicates p < 0.05, ** indicates p < 0.01, **** indicates p < 0.0001. Data are shown as mean \pm SEM. (For interpretation of the references to colour in this figure legend, the reader is referred to the web version of this article.)

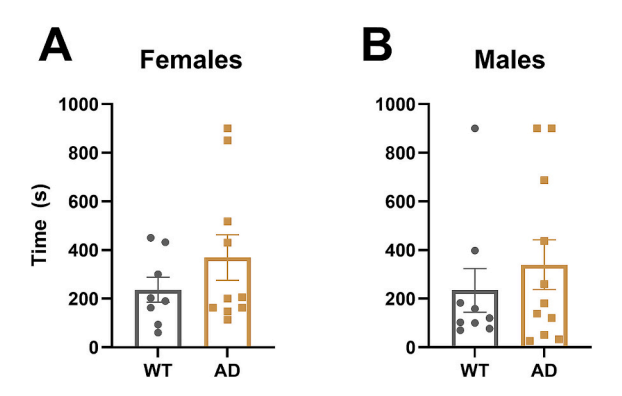


Fig. 4. Total time to find hidden cocoa balls in the hidden food test. There was no difference either between (A) WT (N = 8) and AD (N = 10) female rats or (B) WT (N = 9) and AD (N = 11) male rats, suggesting that olfaction is not impaired in early-stage AD in TgF344-AD rats. Data are shown as mean \pm SEM.

U test when comparing the energy in the given frequency bands in the resting state between WT and AD rats ($p_{delta} = 0.481$, $p_{theta} = 0.20$, $p_{alpha} = 0.277$, $p_{beta} = 0.673$, p_{low} $p_{gamma} = 0.963$, and p_{high} $p_{gamma} = 0.673$). These results suggest that the energy distributions in these frequency bands are similar in both groups (Fig. 8A).

To compare general information processing between WT and AD rats during the resting state, we analyzed the coupling between a slow (theta) phase and the amplitude of a faster oscillation (low gamma, high gamma). Mann-Whitney U test showed no differences for theta-low gamma MI (p = 0.20) and theta-high gamma MI (p = 0.167). These results suggest a similar functional interaction between theta and gamma bands during the resting state in both groups of rats (Fig. 8B).

3.6. Neural activity during 5TSMT and 5TOMT

Before analyzing neural activity during the behavioral tasks, we evaluated the behavior of WT and AD electrophysiological groups of rats during 5TSMT and 5TOMT. Non-significant group (p > 0.14), but significant trial (p < 0.0001) and interaction effects were revealed (p = 0.0011). In both groups, the difference of most trials from the first trial confirms that the subject rats habituated to the first stranger rat (WT: $p_{t1/2}=0.503,\,p_{t1/3}<0.0001,\,p_{t1/4}<0.0001;\,\text{AD:}\,p_{t1/2}=0.1634,\,p_{t1/3}$

= 0.0005, $p_{t1/4}$ = 0.0147). WT rats ($p_{t4/5}$ = 0.0001) but not AD rats ($p_{t4/5}$ > 0.99) increased the interest in the second stranger rat in the fifth trial (Fig. 9). As for 5TOMT, results only showed a significant effect of trial (p = 0.0326) but non-significant group (p > 0.73) and interaction (p > 0.92) effects (Fig. 10). All two-way ANOVA results are reported in Supp. Table 5, post-hoc tests are reported in Supp. Table 2.

As described in Methods, when assessing the neural activity during 5TSMT and 5TOMT, we analyzed only substantial interaction periods to reflect the activity during the processing of information about stranger rats or objects specifically. We focused our analysis on the first and fifth trials in the 5TSMT and 5TOMT. The first trial provided insights into the rats' initial willingness to explore the first stranger rat or object, while the fifth trial reflected their social or object memory retention. Trials 2–4 were primarily utilized to habituate the rats to the presence of the first stranger rat or object.

We did not observe differences in the PSD of individual frequency bands between WT and AD rats during any of the trials, which suggests that the neural dynamics during interactions with novel rats or objects are similar in both groups (Fig. 9A + Supp. Table 3). During the first trial of the 5TSMT, the Mann-Whitney U test showed lower MI for theta-low gamma coupling in AD rats ($p_{t1s}=0.0289$) and no differences in the theta-high gamma MI ($p_{t1s}=0.121$) between the AD and WT groups (Fig. 9B). In addition, we observed equal MI for theta-low gamma coupling in both groups ($p_{t5s}=0.517$) but lower theta-high gamma MI in the AD rats during the fifth trial of the 5TSMT ($p_{t5s}=0.0167$) (Fig. 9C). Our results suggest impaired processing of social stimuli in the AD group.

On the contrary, during the first trial of the 5TOMT, the Mann-Whitney U test showed no differences for theta-low gamma MI ($p_{t1o} = 0.40$) and theta-high gamma MI ($p_{t1o} > 0.99$) (Fig. 10B). Similar results were obtained for the fifth trial of the 5TOMT (theta-low gamma MI: $p_{t5o} = 0.286$, and theta-high gamma MI: $p_{t5o} = 0.111$) (Fig. 10C). These results suggest no effect of genotype on the processing of information about objects.

4. Discussion

Alterations in sociability and social cognition are well-documented in AD patients (Amlerova et al., 2022; Flicker et al., 1990; Jost and Grossberg, 1996; Mazzi et al., 2020; Nelis et al., 2011; Savaskan et al., 2018) as well as mouse AD models (Cheng et al., 2013; Deacon et al.,

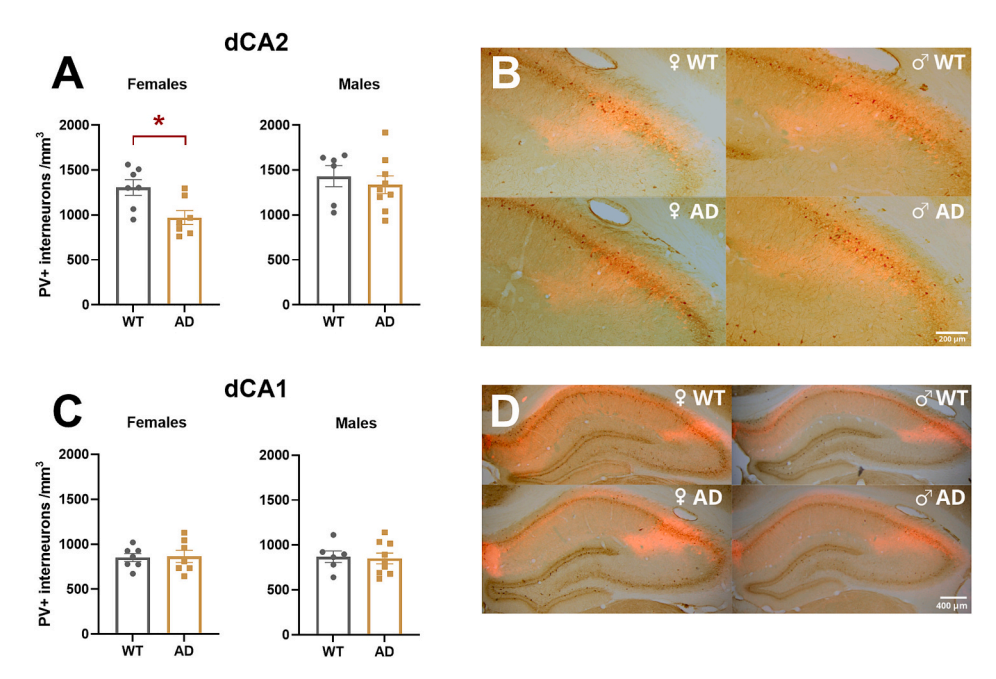


Fig. 5. PV+ interneuron counts in the hippocampal dCA2 (A) and dCA1 (C). Compared to WT (N = 7) females, significant PV loss was observed in AD (N = 7) females in the dCA2 but not in CA1. No difference was observed between WT (N = 6) and AD (N = 9) males in either dCA2 or dCA1. Representative images in B and D show the location of dCA2 (RGS14 staining in red). The count for each rat is a mean of 6 brain hemispheres. * indicates p < 0.05. Data are shown as mean \pm SEM. (For interpretation of the references to colour in this figure legend, the reader is referred to the web version of this article.)

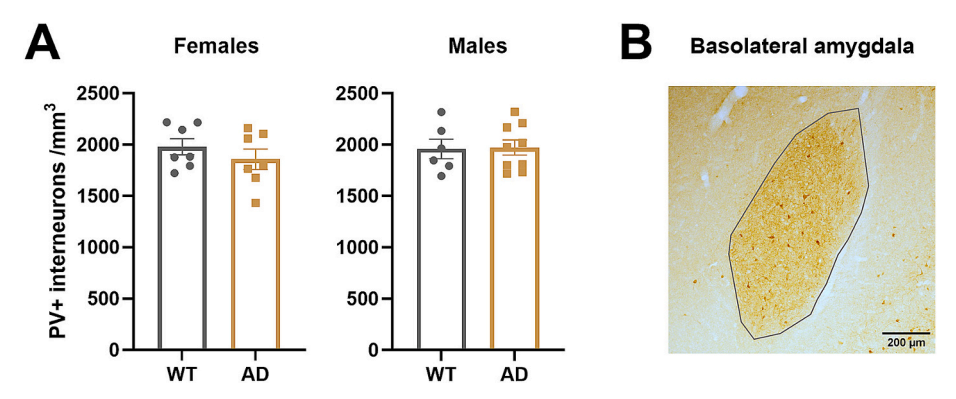


Fig. 6. PV+ interneuron counts in the basolateral amygdala (BLA). No difference was found between WT (N = 7) and AD (N = 7) female rats or between WT (N = 6) and AD (N = 9) male rats (A). A representative image of BLA from a female AD rat is shown in (B). The count for each rat is a mean of 6 brain hemispheres. Data are shown as mean \pm SEM.

2009; Filali et al., 2011; Kosel et al., 2019; Locci et al., 2021; Pietropaolo et al., 2012; Rey et al., 2022), but rarely explored in rat AD models. Previously, our lab assessed social interaction and recognition in McGill-R-Thy1-APP rats, finding qualitative changes but no significant sociability deficits (Petrasek et al., 2018). Moreover, we showed reduced sociability during the simple free social interaction task in TgF344-AD rats at 10 and 14 months (Černotová et al., 2025).

This study is the first to evaluate social cognition in TgF344-AD rats at the early-plaque stage (6 months), emphasizing the hippocampal dCA2, a region critical for social information processing (Hitti and Siegelbaum, 2014; Stevenson and Caldwell, 2014). We used the 5TSMT to assess habituation and social novelty preference. Unlike tests allowing free interaction, this paradigm emphasizes the active social interest of the tested subject. We report robust deficits in sociability and social memory in the TgF344-AD rats, with a sex- and region-dependent reduction of PV+ interneuron number in the dCA2, and impaired theta-gamma phase-amplitude coupling during social interactions.

4.1. Social behavior and memory

Our findings show social interaction deficits in TgF344-AD rats. Both AD males and females exhibited significantly reduced social investigation, aligning with previous reports of diminished sociability during the free-interaction social test in 9- (Chaney et al., 2021), 10- and 14-month old rats (Černotová et al., 2025). The AD males still habituated to the first stranger rat (trials 1–4), whereas AD females did not, possibly due to their low social interest from the test's beginning. Social deficits in early-stage AD mouse models vary, with some studies reporting reduced interest (Cao et al., 2023; Filali et al., 2011; Pietropaolo et al., 2012) and others finding no differences (Kosel et al., 2019; Zhang et al., 2021). Thus, the animal species, transgenic background, and experimental conditions should be considered when investigating social deficits in AD models.

We also report social memory impairment in TgF344-AD rats. Unlike WT rats, which exhibited increased social novelty preference in the fifth trial, AD rats showed no such increase, indicating social recognition deficits (Lemaire, 2003). This aligns with most findings in various

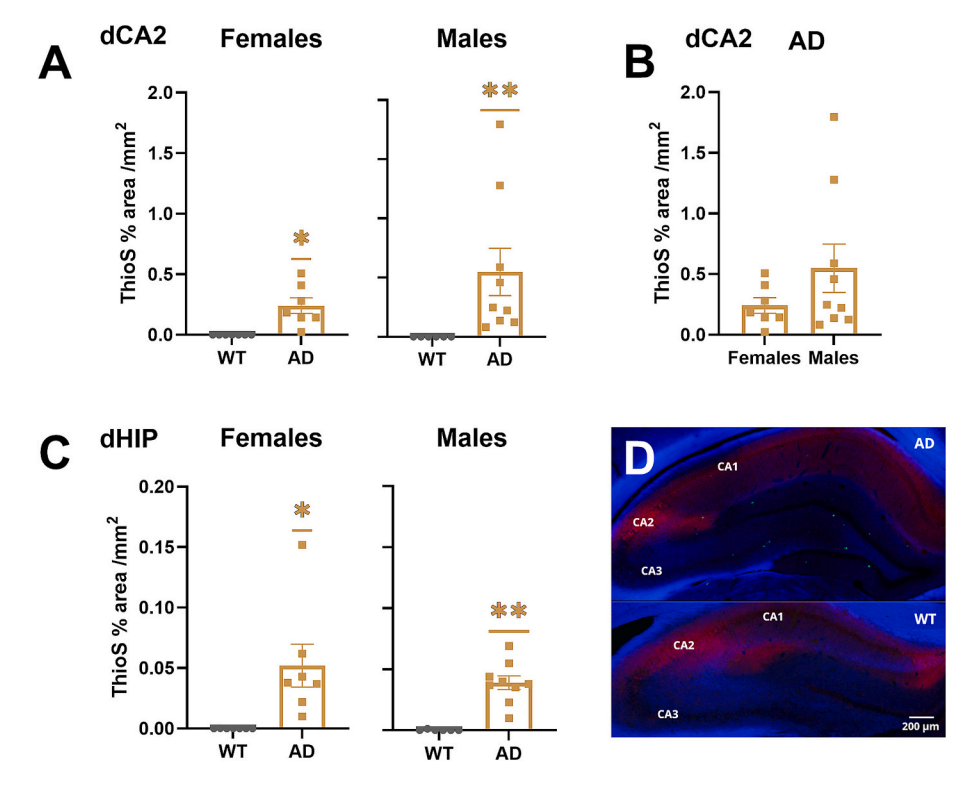


Fig. 7. The β -amyloid plaque load in the dCA2 (A) and whole dorsal hippocampus (C), with statistical analysis confirming a significant difference from zero in AD rats. The % amount of plaques did not differ between male and female AD rats in the dCA2 (B). A representative image of the dorsal hippocampus is seen in (D); plaques are visualized in green (ThioS), and dCA2 is visualized in red (RGS14). The count for each rat is a mean of 6 brain hemispheres. * indicates p < 0.05, ** indicates p < 0.01. Data are shown as mean \pm SEM. (For interpretation of the references to colour in this figure legend, the reader is referred to the web version of this article.)

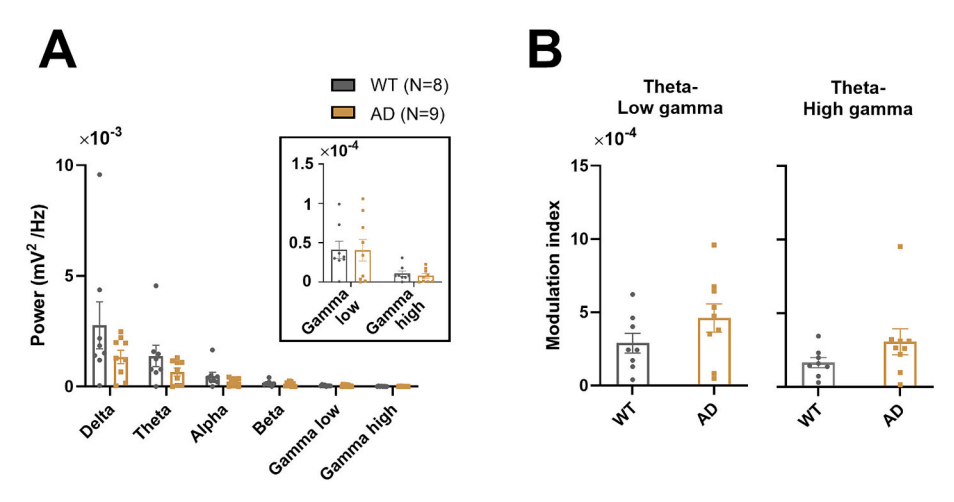


Fig. 8. Resting state neural activity. There were no differences in the power of the given frequency bands (A) or the theta-low gamma and theta-high gamma coupling (B) in the resting state between the WT and AD rats. Data are shown as mean \pm SEM.

transgenic AD mouse models (Cao et al., 2023; Filali et al., 2011; Misrani et al., 2021; Perusini et al., 2017; Várkonyi et al., 2022; Zhang et al., 2021). The only exception we are aware of is a study on 5xFAD female mice, reporting intact social novelty preference at 6 months (Kosel et al., 2019).

Hyposmia may accompany early-stage AD (Roberts et al., 2016) and negatively affect social recognition (Pena et al., 2014); surprisingly, this is rarely addressed in studies related to social memory. We conducted a hidden food test to rule out olfactory deficits as a confounder, confirming intact olfaction in TgF344-AD rats. Previous studies showed olfactory impairment in AD models (Li et al., 2019; Mitrano et al., 2021; Saré et al., 2020). Our results contrast with that of Saré et al. (2020),

who found genotype effects in TgF344-AD males at 6, 12, and 18 months. The study had a smaller sample size, and most rats reached the maximum test duration of 900 s (3 out of 4 AD male rats at 6 months of age). In contrast, only 2 of 11 AD male rats in our study reached the maximum limit. Additionally, we used chocolate balls in the task, along with prior habituation. The specific food and task conditions were not reported in the study of Saré et al.

Anxiety and reduced exploratory drive could also affect social interest and recognition. Previous studies reported anxiety-like behavior in TgF344-AD rats (Lopez et al., 2024; Pentkowski et al., 2018; Srivastava et al., 2023; Tournier et al., 2021) and hypoactivity in TgF344-AD females (Saré et al., 2020; Srivastava et al., 2023). Indeed, our pilot

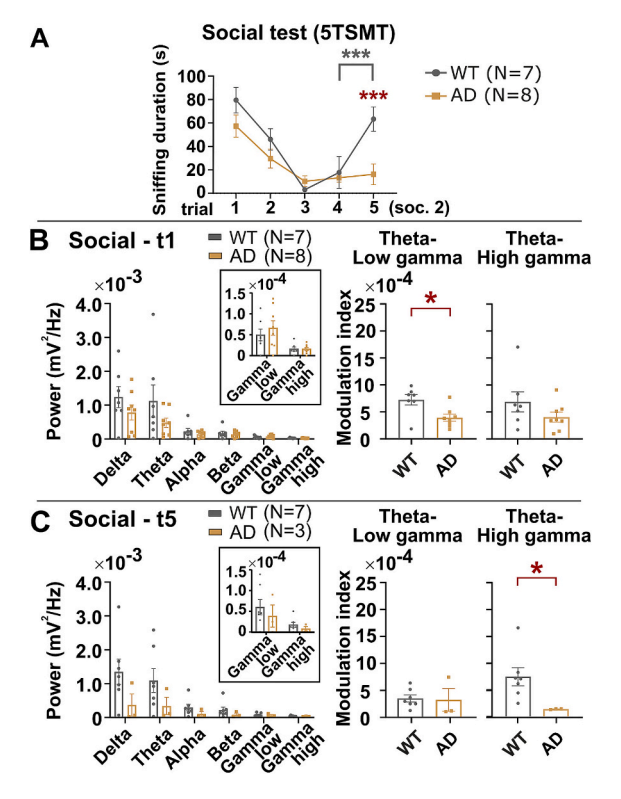


Fig. 9. 5TSMT behavioral results from the LFP-recorded males (A) and corresponding electrophysiological results in social trials 1 and 5 (B-C). There was a significant effect of trial and interaction in the 5TSMT (A). Habituation to the first stranger rat across trials was confirmed in both groups, with WT but not AD rats showing increased interest in the second stranger rat in the fifth trial. There were no differences in the PSD of individual frequency bands between WT and AD rats during interactions with novel rats, indicating similar neural dynamics in both groups (B-C). However, during the 5TSMT, AD rats exhibited lower theta-low gamma and theta-high gamma coupling during the first and fifth trials, respectively, suggesting impaired processing of social stimuli compared to WT rats. Significant differences between WT and AD groups are indicated by red asterisks, while significant differences between trials 4 and 5 within WT groups are marked by grey asterisks. Detailed post-hoc results for trials are provided in the text and Supp. Table 2. All PSD results from trials 1 and 5 are shown in Supp. Table 3. * indicates p < 0.05, ** indicates p < 0.01, *** indicates p < 0.001. Data are shown as mean \pm SEM. (For interpretation of the references to colour in this figure legend, the reader is referred to the web version of this article.)

experiments suggested reduced motivation to explore caged rats in other environments (data not shown). Social behavior was maximized by performing the 5TSMT in rats' home cages. All rats in our experiment investigated the first stranger rat in trial 1 and had the same conditions for the subsequent "habituation" trials. WT rats of both sexes exhibited a strong preference for social novelty, confirming the reliability of our test. Although we cannot definitively determine whether the lack of social novelty preference in AD rats or habituation in AD females was due to anxiety, apathy, or a deficit in social recognition, our subsequent electrophysiological experiment revealed alterations in brain oscillatory patterns during social investigation, suggesting a broader impairment in social information processing.

4.2. PV+ interneurons

Numerous rodent studies have reported early morphological and functional changes in PV+ interneurons in rodent AD models (Černotová et al., 2023). Recent proteomic analyses by Kumar et al. (2024) revealed significant alterations in these interneurons, consistent across the 5xFAD mouse model and human AD patients. Notably, they

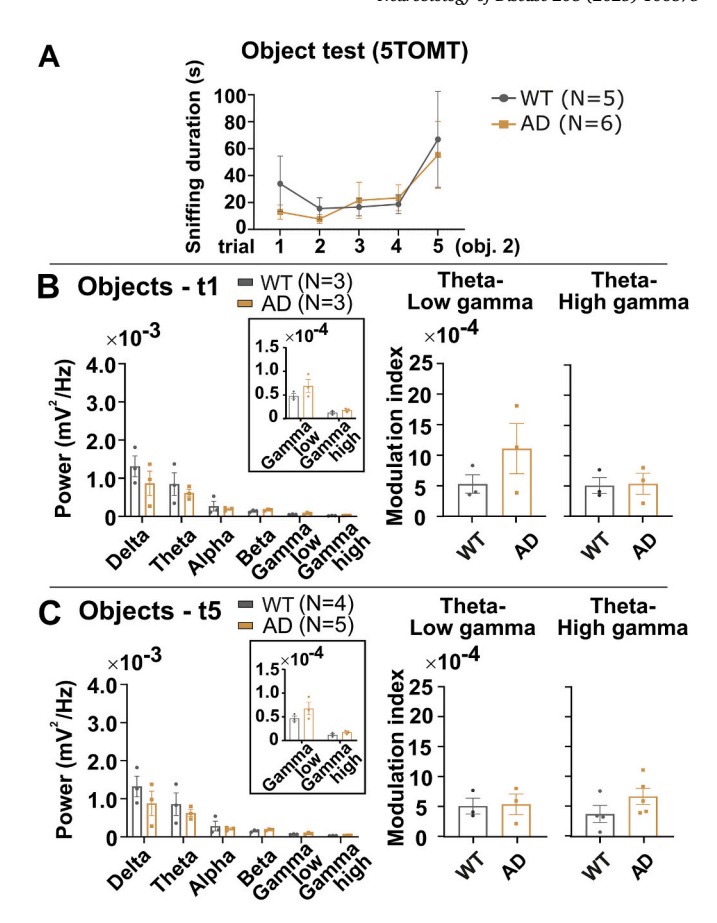


Fig. 10. 5TOMT behavioral results from the LFP-recorded males (A) and corresponding electrophysiological results in object trials 1 and 5 (B–C). The behavioral analysis only showed a significant effect of trial but non-significant group and interaction effects (A). There were no differences in the PSD of individual frequency bands between WT and AD rats during interactions with objects, indicating no genotype effect on object information processing (B–C). Data are shown as mean \pm SEM. All PSD results from trials 1 and 5 are shown in Supp. Table 3.

found a correlation between decreased PV+ interneuron-associated proteins, progressing neuropathology and cognitive decline.

While PV+ interneuron dysfunction has been linked to social behavior deficits in autism models (Shih et al., 2023; Tatsukawa et al., 2018), its role in AD remains unclear. Rey et al. (2022) is the only study to directly examine this connection, reporting social memory impairment and PV+ interneuron loss in the dCA2 of 9-month-old Tg2576 mice. Restoring perineural nets of PV+ interneurons by injecting the growth factor neuregulin-1 to the dCA2 rescued social memory.

Our study discovered a sex- and region-specific decline in PV+ interneurons in the dCA2 at 6 months, with AD females showing a distinct reduction in PV+ interneuron cells. The specificity of this finding is highlighted by the absence of PV+ cell reduction in the dCA1 and BLA. The dCA1 is traditionally associated with object discrimination and spatial memory (Stackman et al., 2016), while dCA2 is critical for encoding social novelty and processing social memory (Hitti and Siegelbaum, 2014; Stevenson and Caldwell, 2014; Donegan et al., 2020). Although BLA is involved in social cognition, it primarily contributes to social exploration and determining social salience rather than discrimination between individuals (Fustiñana et al., 2021; Maaswinkel et al., 1996; Song et al., 2021). Our findings suggest that PV+ interneuron loss in the dCA2 contributes to the reduced social interest and lack of habituation in AD females during the 5TSMT. This aligns with previous research showing GABAergic cell loss in the CA1 of 9-month-old sexbalanced TgF344-AD rats (Bazzigaluppi et al., 2018) and a reduced

number of PV+ interneurons in the dCA2/3 of 9-month-old, but not 6-month-old males (Sun, 2023).

Our results also comply with evidence highlighting greater susceptibility to AD pathology in females, observed in both human (Barnes et al., 2005) and rodent studies (Berkowitz et al., 2018; Chaudry et al., 2022; Jiao et al., 2016; Poon et al., 2023; Yang et al., 2018). PV+ interneurons are particularly vulnerable to metabolic and oxidative stress and hormonal fluctuations (Ruden et al., 2021; Terstege and Epp, 2023). While female TgF344-AD rats show higher neuronal density in the hippocampus at 9 months – potentially due to estrogen's neuroprotective effects – they simultaneously display increased β -amyloid load and reactive microglia (Chaudry et al., 2022).

Importantly, our observation of PV+ interneuron loss appears independent of the typical AD pathology. Our rats had low β -amyloid plaque load at 6 months, consistent with Cohen et al. (2013), and no sex differences in pathology at this age. Tau pathology in the hippocampus typically emerges later, around 16–18 months (Cohen et al., 2013; Rorabaugh et al., 2017; Chaney et al., 2021). Given that AD female rats exhibit anxiety- and depressive-like behaviors (Lopez et al., 2024; Pentkowski et al., 2018; Srivastava et al., 2023; Tournier et al., 2021), the interplay of disease progression, behavioral alterations, and hormonal fluctuations may drive PV+ interneuron vulnerability, contributing to accelerated pathology.

Our histological evaluations were performed after behavioral testing, which may influence PV+ interneuron expression. Donato et al. (2013) demonstrated that interneurons exist in low-PV to high-PV states depending on environmental and learning experiences, without affecting total cell count. We included both low-PV and high-PV cells in counting; thus, the reduced count of PV+ interneurons in AD female rats likely reflects actual numerical reduction. However, we cannot determine whether this reduction is due to actual neuronal death or loss of PV protein expression – two distinct processes with different functional consequences. Loss of PV protein leads to interneuron hyperexcitability, whereas loss of PV+ interneurons reduces inhibition, causing hyperexcitation of brain regions (Filice et al., 2016).

Some researchers propose that PV+ interneurons initially become hyperexcitable, followed by chronic depletion with hypofunction, ultimately accelerating AD progression (Algamal et al., 2022; Hijazi et al., 2020). Supporting this, Kumar et al. (2024) identified increased mitochondrial, synaptic, and metabolic proteins in PV+ interneurons during early disease stages. While our current study does not address these mechanisms, it highlights the need for future research to explore PV+ interneuron hyperactivation and protein expression as potential markers of early AD pathophysiology.

4.3. Hippocampal oscillations

Brain oscillations play a critical role in numerous cognitive processes, which are often impaired in neurological diseases, and recent studies have increasingly focused on the interactions between multiple rhythms, particularly on the theta-gamma phase-amplitude coupling (PAC) – a mechanism proposed to have a key role in information processing and interregional communication (Colgin, 2015). Although the male AD rats in our study did not show changes in PV+ interneurons in the dCA2 area, they did show apparent social behavior deficits in the 5TSMT. Therefore, it is of interest to study the electrophysiological patterns in the hippocampus of these rats to possibly reveal impairments in brain oscillations that may precede the actual loss of PV+ interneurons.

The behavior of the electrophysiological group of male rats during the 5TSMT was similar to that of unimplanted male AD and WT rats. Both genotypes showed habituation to the first stranger rat (trials 1–4), though only the WT group demonstrated increased interest in the second stranger rat in trial 5. As for 5TOMT, which was only performed in the electrophysiological group, the experimental rats showed substantially lower interest in objects than stranger rats, resulting in fewer subjects

exploring during the 5TOMT. Since the analysis lacked statistical significance for a difference in habituation or novel object preference, we cannot draw firm conclusions from the behavioral results of this test. Despite these limitations, some lines of evidence support our conclusion of specific social deficits in AD rats: We observed no significant betweengroup differences in the 5TOMT, contrasting with the clear AD-related deficits in novel rat exploration in the 5TSMT. Moreover, the analysis of electrophysiological recordings confirmed preserved brain oscillations during object exploration while showing distinct abnormalities in the social task. These findings suggest that the cognitive impairment in our AD model preferentially affects social processing pathways rather than overall novelty detection or exploratory behavior.

We note a trend towards decreased energy levels in the dCA2 activity in AD rats, particularly within the theta-alpha frequency bands (4–10 and 10–13 Hz). Despite this trend, no significant differences were observed. Previous electrophysiological studies were conducted solely in the dCA1 and TgF344-AD rats at an earlier age (4–5 months) displayed reduced power in the high theta range (8–12 Hz) during an open field test, potentially influenced by novelty and stress as this decrease was not as pronounced during a repeated test the following day (van den Berg et al., 2023). Furthermore, at 6 months, there was a non-significant trend towards reduced brainstem-elicited hippocampal theta (3–9 Hz) oscillations under anesthesia, with a significant decrease in the lower theta range (Stoiljkovic et al., 2019).

Additionally, reductions in both low (30-50 Hz) and high gamma (50-100 Hz) oscillations were observed during exploration on a linear track in 6-month-old TgF344-AD rats (Moradi et al., 2023). Although this study offers interesting insights, we question its statistical methods. As TgF344-AD rats aged, more pronounced alterations in hippocampal oscillations emerged. At 9 to 12 months, there was a clear decline in elicited hippocampal theta (3-9 Hz) oscillations under anesthesia. Similarly, in freely moving rats aged 9-12 months, reductions in hippocampal theta activity were observed (Stoiljkovic et al., 2019). In another study, TgF344-AD rats aged 8-9 months attenuated in the low gamma band (30-58 Hz) under sedation (Bazzigaluppi et al., 2018). These findings underscore age-related changes in hippocampal oscillations in the TgF344-AD rat model. While subtle differences in PSD of individual brain rhythms were noted in the pre-plaque stages (<6 months of age) of TgF344-AD rats, clear distinctions emerged in older animals, particularly in hippocampal theta and gamma oscillations, which are crucial for cognitive functions and information processing. The activity of PV+ interneurons plays a key role in the generation of theta and gamma oscillations in the hippocampus, and changes in their activity can lead to changes in both rhythms as well as the coupling between them (Amilhon et al., 2015; Bartos et al., 2007; Park et al., 2020). Although we did not observe changes in the number of PV+ interneurons in male AD rats, their activity may be altered in the earlystage AD, leading to subtle impairments in brain rhythm interactions, such as PAC between theta and gamma.

Theta-gamma PAC in the CA2 region has been shown to be crucial for distinguishing between novel and familiar social stimuli, as well as for retrieving remote social memories in mice (Laham et al., 2024). In addition, the inhibition of CA2 has been shown to reduce low gamma power in CA1, specifically during novel social but not object interactions (Brown et al., 2020). Consistent with the role of dCA2 in social information processing, we observed a decrease in theta-gamma PAC in hippocampal dCA2, specifically during direct social interactions in the 5TSMT but not during the 5TOMT, where rats interacted with objects. We show reduced theta-low gamma PAC during the first trial of 5TSMT, which primarily addresses sociability and the willingness of rats to start social interactions with unfamiliar subjects, and reduced theta-high gamma PAC during the fifth trial of 5TSMT which reflects social memory and the ability to recognize a novel rat from a familiar one.

Reduced theta-gamma PAC in dCA2 during social interactions may indicate impairments in synchronizing hippocampal networks essential for encoding and recalling social memories. Specifically, disruptions in theta-low gamma PAC could reflect compromised local computations within dCA2, while reductions in theta-high gamma PAC might signify impaired communication with downstream regions, such as the prefrontal cortex. These deficits may underlie the social memory impairments observed in the 5TSMT. Consistent with the role of theta-low gamma PAC in facilitating item-context associations (Tort et al., 2009) and theta-high gamma PAC in recognition memory by synchronizing hippocampal activity with other brain regions like the prefrontal cortex (Alemany-González et al., 2020). These findings suggest that theta-gamma PAC in dCA2 acts as a mechanistic link between hippocampal oscillatory dynamics and social behavior, offering a potential early biomarker for social deficits associated with AD pathology.

Previous studies addressed hippocampal theta-gamma PAC in TgF344-AD rats in the dCA1. Van den Berg et al. (2023) showed reduced PAC between theta (6.5-9.5 Hz) and high gamma (60-90 Hz) during wake immobility but not during active exploration in the open field test in 4- to 5-month-old TgF344-AD rats. However, only during the first day of an open field test, not the repeated test the day after (van den Berg et al., 2023). While comparable at six months, theta-gamma PAC was attenuated in both low (30-55 Hz) and high gamma (65-95 Hz) bands in 12-month-old TgF344-AD rats under urethane anesthesia with elicited hippocampal oscillations (Stoiljkovic et al., 2019). Moradi et al. (2023) reported a significant reduction in both low gamma (30-50 Hz) and high gamma (50-100 Hz) PAC in 6-month-old TgF344-AD rats. However, as mentioned above, we question the statistical methods used in this study. Specifically, their analysis was based on recording sessions rather than representing each animal by a single aggregate measure, which may have inflated the apparent sample size. Additionally, individual animals underwent varying numbers of recording sessions, yet all sessions were included in the analysis without properly accounting for this imbalance in the statistical test. Lastly, the average PAC of theta (3-9 Hz) to highgamma (62-120 Hz) was significantly reduced in 8- to 9-month-old TgF344-AD rats in a sedative resting state (Bazzigaluppi et al., 2018).

In summary, the impairments in theta-gamma PAC are more evident in older animals when recorded during resting states and not consistently observable in younger ($\leq\!6$ months) rats exploring an environment. Impaired cross-frequency modulation of gamma amplitude by theta phase before A β accumulation in some AD mouse models (Goutagny et al., 2013; Ittner et al., 2014) suggests that altered theta-gamma PAC may represent an early biomarker in AD pathology. We are the first to report theta-gamma PAC measures and specific impairments in TgF344-AD rats during a social memory task.

Sex-specific alterations in the medial perforant pathway in 6-monthold males but not in females have been observed in TgF344-AD rats (Smith and McMahon, 2018). In contrast, we observed PV+ interneuron loss in the dCA2 region of 6-month-old females but not males. Interestingly, male rats exhibited PAC deficits in the dCA2 during social tasks, suggesting network-level disruptions independent of PV+ interneuron loss. While we did not record electrophysiological data in females, similar PAC impairments may occur, given their interneuron loss. These findings suggest distinct, sex-specific vulnerabilities across hippocampal pathways, emphasizing the need to explore how different regions and mechanisms contribute to AD pathology.

5. Limitations of the study

A minor limitation in this study was our focus on PV+ interneuron counts without considering PV protein expression levels within individual cells. It would be interesting to look at how social interactions affect the PV amount in the cells and if this transition is somehow affected in AD animals. The second limitation is that the 5TOMT was performed only with the implanted rats. Including the 5TOMT in our initial behavioral experiments may have further supported the specificity of the observed social deficits. However, the implanted rats exhibited an unexpected lack of object interaction, and it is questionable whether the non-implanted cohort would have shown more interest. The

low interest of rats in objects constrained our ability to evaluate oscillatory patterns during social versus non-social interactions in a large group of rats. We also limited electrophysiology to the exclusive use of male subjects, given their previous standard behavior in the 5TSMT. Including females would have been particularly valuable given the observed PV+ interneuron impairments, although it would likely require additional social testing paradigms. Future studies should explore broader questions about how social information is processed in AD, examine potential alterations in other interneuron populations, and investigate whether targeted modulation of associated social circuits could potentially ameliorate AD-related social deficits. In view of our results, it is essential to address further the differences between male and female individuals.

6. Conclusion

Our study shows that decreased social interest and social memory impairment belong to the first behavioral symptoms in TgF344-AD rats and confirms that the social deficits are similar to AD patients. Our results revealed a sex- and region-specific reduction in the number of PV+ interneurons, with females being more affected and showing a decrease in PV+ interneurons in the hippocampal dCA2. We further showed alterations in theta-gamma phase-amplitude coupling in the hippocampal dCA2 during interactions with other rats but not objects, indicating selective impairments in social information processing. Together, these results offer novel insights into the early changes in social behavior and dCA2 oscillations in TgF344-AD rats.

CRediT authorship contribution statement

Daniela Černotová: Writing – review & editing, Writing – original draft, Visualization, Validation, Project administration, Methodology, Investigation, Funding acquisition, Formal analysis, Data curation, Conceptualization. Karolína Hrůzová: Writing – review & editing, Visualization, Methodology, Investigation, Conceptualization. Jan Touš: Software, Formal analysis. Radek Janča: Writing – review & editing, Visualization, Software. Aleš Stuchlík: Writing – review & editing, Supervision, Funding acquisition, Conceptualization. David Levčík: Writing – review & editing, Writing – original draft, Validation, Supervision, Project administration, Methodology, Conceptualization. Jan Svoboda: Writing – review & editing, Supervision, Project administration, Funding acquisition, Conceptualization.

Declaration of Generative AI and AI-assisted technologies in the writing process

During the preparation of this work the authors used ChatGPT-3.5 and Claude 3.5 Sonnet to improve the readability and language of the manuscript. After using this tool/service, the authors reviewed and edited the content as needed and take full responsibility for the content of the published article.

Funding sources

This study was supported by the Czech Science Foundation (GACR), first by grant 21-16667K (awarded to AS), followed by grant 25-16227S (awarded to JS). Further support was provided by the National Institute for Neurology Research (Programme EXCELES, ID Project No. LX22NPO5107), funded by the European Union–Next Generation EU. Daniela Černotová and Karolína Hrůzová acknowledge support by the student project Grant Schemes at Charles University, reg. no. CZ.02.2.69/0.0/0.0/19 073/0016935. Jan Touš and Radek Janča were supported by the Grant Agency of the Czech Technical University in Prague (SGS23/170/OHK3/3T/13).

Declaration of competing interest

The authors declare that they have no known competing financial interests or personal relationships that could have appeared to influence the work reported in this paper.

Appendix A. Supplementary data

Supplementary data to this article can be found online at https://doi.org/10.1016/j.nbd.2025.106875.

Data availability

Data will be made available on request.

References

- Alemany-González, M., Gener, T., Nebot, P., Vilademunt, M., Dierssen, M., Puig, M.V., 2020. Prefrontal-hippocampal functional connectivity encodes recognition memory and is impaired in intellectual disability. Proc. Natl. Acad. Sci. USA 117, 11788. https://doi.org/10.1073/pnas.1921314117.
- Algamal, M., Russ, A.N., Miller, M.R., Hou, S.S., Maci, M., Munting, L.P., Zhao, Q., Gerashchenko, D., Bacskai, B.J., Kastanenka, K.V., 2022. Reduced excitatory neuron activity and interneuron-type-specific deficits in a mouse model of Alzheimer's disease. Commun. Biol. 5. https://doi.org/10.1038/S42003-022-04268-X.
- Amilhon, B., Huh, C.Y.L., Manseau, F., Ducharme, G., Nichol, H., Adamantidis, A., Williams, S., 2015. Parvalbumin interneurons of hippocampus tune population activity at theta frequency. Neuron 86, 1277–1289. https://doi.org/10.1016/J. NEURON.2015.05.027.
- Amlerova, J., Laczó, J., Nedelska, Z., Laczó, M., Vyhnálek, M., Zhang, B., Sheardova, K., Angelucci, F., Andel, R., Hort, J., 2022. Emotional prosody recognition is impaired in Alzheimer's disease. Alzheimers Res. Ther. 14. https://doi.org/10.1186/S13195-022-00989-7.
- Barnes, L.L., Wilson, R.S., Bienias, J.L., Schneider, J.A., Evans, D.A., Bennett, D.A., 2005. Sex differences in the clinical manifestations of Alzheimer disease pathology. Arch. Gen. Psychiatry 62, 685–691. https://doi.org/10.1001/ARCHPSYC.62.6.685.
- Bartos, M., Vida, I., Jonas, P., 2007. Synaptic mechanisms of synchronized gamma oscillations in inhibitory interneuron networks. Nat. Rev. Neurosci. 8, 45–56. https://doi.org/10.1038/NRN2044.
- Bazzigaluppi, P., Beckett, T.L., Koletar, M.M., Lai, A.Y., Joo, I.L., Brown, M.E., Carlen, P. L., McLaurin, J.A., Stefanovic, B., 2018. Early-stage attenuation of phase-amplitude coupling in the hippocampus and medial prefrontal cortex in a transgenic rat model of Alzheimer's disease. J. Neurochem. 144, 669–679. https://doi.org/10.1111/ JNC.14136.
- Berkowitz, L.E., Harvey, R.E., Drake, E., Thompson, S.M., Clark, B.J., 2018. Progressive impairment of directional and spatially precise trajectories by TgF344-Alzheimer's disease rats in the Morris Water Task. Sci. Rep. 8, 16153. https://doi.org/10.1038/ s41598-018-34368-w.
- Botcher, N.A., Falck, J.E., Thomson, A.M., Mercer, A., 2014. Distribution of interneurons in the CA2 region of the rat hippocampus. Front. Neuroanat. 8. https://doi.org/10.3389/FNANA.2014.00104.
- Brady, D.R., Mufson, E.J., 1997. Parvalbumin-immunoreactive neurons in the hippocampal formation of Alzheimer's diseased brain. Neuroscience 80, 1113–1125. https://doi.org/10.1016/S0306-4522(97)00068-7.
- Brown, L.Y., Alexander, G.M., Cushman, J., Dudek, S.M., 2020. Hippocampal CA2 organizes CA1 slow and fast γ oscillations during novel social and object interaction. eNeuro 7. https://doi.org/10.1523/ENEURO.0084-20.2020.
- Cao, Q., Kumar, M., Frazier, A., Williams, J.B., Zhao, S., Yan, Z., 2023. Longitudinal characterization of behavioral, morphological and transcriptomic changes in a tauopathy mouse model. Aging (Albany NY) 15, 11697. https://doi.org/10.18632/ AGING.205057.
- Černotová, D., Hrůzová, K., Levčík, D., Svoboda, J., Stuchlík, A., 2023. Linking social cognition, Parvalbumin interneurons, and oxytocin in Alzheimer's disease: an update. J. Alzheimers Dis. 96, 861. https://doi.org/10.3233/JWT230333.
- Černotová, D., Malenínská, K., Horáková, A., Stuchlík, A., Svoboda, J., 2025. Social Interaction Deficits Emerge Alongside Anxiety-like Behavior in TgF344-AD Rats. Authorea [Preprint]. https://doi.org/10.22541/au.173929882.27357606/v1.
- Chaney, A.M., Lopez-Picon, F.R., Serrière, S., Wang, R., Bochicchio, D., Webb, S.D., Vandesquille, M., Harte, M.K., Georgiadou, C., Lawrence, C., Busson, J., Vercouillie, J., Tauber, C., Buron, F., Routier, S., Reekie, T., Snellman, A., Kassiou, M., Rokka, J., Davies, K.E., Rinne, J.O., Salih, D.A., Edwards, F.A., Orton, L. D., Williams, S.R., Chalon, S., Boutin, H., 2021. Prodromal neuroinflammatory, cholinergic and metabolite dysfunction detected by PET and MRS in the TgF344-AD transgenic rat model of AD: a collaborative multi-modal study. Theranostics 11, 6644. https://doi.org/10.7150/THNO.56059.
- Chaudry, O., Ndukwe, K., Xie, L., Figueiredo-Pereira, M., Serrano, P., Rockwell, P., 2022. Females exhibit higher GluA2 levels and outperform males in active place avoidance despite increased amyloid plaques in TgF344-Alzheimer's rats. Sci. Rep. 12, 19129. https://doi.org/10.1038/S41598-022-23801-W.
- Cheng, D., Logge, W., Low, J.K., Garner, B., Karl, T., 2013. Novel behavioural characteristics of the APPSwe/PS1ΔE9 transgenic mouse model of Alzheimer's

- disease. Behav. Brain Res. 245, 120–127. https://doi.org/10.1016/j.
- Cohen, R.M., Rezai-Zadeh, K., Weitz, T.M., Rentsendorj, A., Gate, D., Spivak, I., Bholat, Y., Vasilevko, V., Glabe, C.G., Breunig, J.J., Rakic, P., Davtyan, H., Agadjanyan, M.G., Kepe, V., Barrio, J.R., Bannykh, S., Szekely, C.A., Pechnick, R.N., Town, T., 2013. A transgenic alzheimer rat with plaques, tau pathology, behavioral impairment, oligomeric Δβ, and frank neuronal loss. J. Neurosci. 33, 6245–6256. https://doi.org/10.1523/JNEUROSCI.3672-12.2013.
- Colgin, L.L., 2015. Theta-gamma coupling in the entorhinal-hippocampal system. Curr. Opin. Neurobiol. 31, 45–50. https://doi.org/10.1016/J.CONB.2014.08.001.
- Deacon, R.M.J., Koros, E., Bornemann, K.D., Rawlins, J.N.P., 2009. Aged Tg2576 mice are impaired on social memory and open field habituation tests. Behav. Brain Res. 197, 466–468. https://doi.org/10.1016/J.BBR.2008.09.042.
- Do Carmo, S., Cuello, A., 2013. Modeling Alzheimer's disease in transgenic rats. Mol. Neurodegener. 8, 37. https://doi.org/10.1186/1750-1326-8-37.
- Donato, F., Rompani, S.B., Caroni, P., 2013. Parvalbumin-expressing basket-cell network plasticity induced by experience regulates adult learning. Nature 504, 272–276. https://doi.org/10.1038/NATURE12866.
- Donegan, M.L., Stefanini, F., Meira, T., Gordon, J.A., Fusi, S., Siegelbaum, S.A., 2020. Coding of social novelty in the hippocampal CA2 region and its disruption and rescue in a 22q11.2 microdeletion mouse model. Nat. Neurosci. 23, 1365–1375. https://doi.org/10.1038/S41593-020-00720-5.
- Dong, H., Goico, B., Martin, M., Csernansky, C.A., Bertchume, A., Csernansky, J.G., 2004. Modulation of hippocampal cell proliferation, memory, and amyloid plaque deposition in APPsw (Tg2576) mutant mice by isolation stress. Neuroscience 127, 601–609. https://doi.org/10.1016/j.neuroscience.2004.05.040.
- Filali, M., Lalonde, R., Rivest, S., 2011. Anomalies in social behaviors and exploratory activities in an APPswe/PS1 mouse model of Alzheimer's disease. Physiol. Behav. 104, 880–885. https://doi.org/10.1016/j.physbeh.2011.05.023.
- Filice, F., Vörckel, K.J., Sungur, A.Ö., Wöhr, M., Schwaller, B., 2016. Reduction in parvalbumin expression not loss of the parvalbumin-expressing GABA interneuron subpopulation in genetic parvalbumin and shank mouse models of autism. Mol. Brain 9. https://doi.org/10.1186/S13041-016-0192-8.
- Flicker, C., Ferris, S.H., Crook, T., Bartus, R.T., 1990. Impaired facial recognition memory in aging and dementia. Alzheimer Dis. Assoc. Disord. 4, 43–54. https://doi. org/10.1097/00002093-199040100-00005.
- Friard, O., Gamba, M., 2016. BORIS: a free, versatile open-source event-logging software for video/audio coding and live observations. Methods Ecol. Evol. 7, 1325–1330. https://doi.org/10.1111/2041-210X.12584.
- Fustiñana, M.S., Eichlisberger, T., Bouwmeester, T., Bitterman, Y., Lüthi, A., 2021. State-dependent encoding of exploratory behaviour in the amygdala. Nature 592, 267–271. https://doi.org/10.1038/S41586-021-03301-Z.
- Goutagny, R., Gu, N., Cavanagh, C., Jackson, J., Chabot, J.G., Quirion, R., Krantic, S., Williams, S., 2013. Alterations in hippocampal network oscillations and theta–gamma coupling arise before Aβ overproduction in a mouse model of Alzheimer's disease. Eur. J. Neurosci. 37, 1896–1902. https://doi.org/10.1111/EJN.12233.
- Hijazi, S., Heistek, T.S., Scheltens, P., Neumann, U., Shimshek, D.R., Mansvelder, H.D., Smit, A.B., van Kesteren, R.E., 2020. Early restoration of parvalbumin interneuron activity prevents memory loss and network hyperexcitability in a mouse model of Alzheimer's disease. Mol. Psychiatry 25, 3380–3398. https://doi.org/10.1038/ s41380-019-0483-4.
- Hitti, F.L., Siegelbaum, S.A., 2014. The hippocampal CA2 region is essential for social memory. Nature 508, 88–92. https://doi.org/10.1038/nature13028.
- Hsiao, K., Chapman, P., Nilsen, S., Eckman, C., Harigaya, Y., Younkin, S., Yang, F., Cole, G., 1996. Correlative memory deficits, Aβ elevation, and amyloid plaques in transgenic mice. Science (80-.) 274, 99–102. https://doi.org/10.1126/
- Huang, H., Wang, L., Cao, M., Marshall, C., Gao, J., Xiao, N., Hu, G., Xiao, M., 2015. Isolation housing exacerbates Alzheimer's disease-like pathophysiology in aged APP/PS1 mice. Int. J. Neuropsychopharmacol. 18, 1–10. https://doi.org/10.1093/ 11NP/PVII.116
- Ittner, A.A., Gladbach, A., Bertz, J., Suh, L.S., Ittner, L.M., 2014. p38 MAP kinase-mediated NMDA receptor-dependent suppression of hippocampal hypersynchronicity in a mouse model of Alzheimer's disease. Acta Neuropathol. Commun. 2. https://doi.org/10.1186/S40478-014-0149-Z.
- Jiao, S.S., Le Bu, X., Liu, Y.H., Zhu, C., Wang, Q.H., Shen, L.L., Liu, C.H., Wang, Y.R., Yao, X.Q., Wang, Y.J., 2016. Sex dimorphism profile of Alzheimer's disease-type pathologies in an APP/PS1 mouse model. Neurotox. Res. 29, 256–266. https://doi.org/10.1007/S12640-015-9589-X/METRICS.
- Jost, B.C., Grossberg, G.T., 1996. The evolution of psychiatric symptoms in Alzheimer's disease: a natural history study. J. Am. Geriatr. Soc. 44, 1078–1081. https://doi.org/ 10.1111/j.1532-5415.1996.tb02942.x.
- Ko, J., 2017. Neuroanatomical substrates of rodent social behavior: the medial prefrontal cortex and its projection patterns. Front. Neural Circuits 11, 276485. https://doi. org/10.3389/FNCIR.2017.00041/BIBTEX.
- Kosel, F., Torres Munoz, P., Yang, J.R., Wong, A.A., Franklin, T.B., 2019. Age-related changes in social behaviours in the 5xFAD mouse model of Alzheimer's disease. Behav. Brain Res. 362, 160–172. https://doi.org/10.1016/J.BBR.2019.01.029.
- Kumar, P., Goettemoeller, A.M., Espinosa-Garcia, C., Tobin, B.R., Tfaily, A., Nelson, R.S., Natu, A., Dammer, E.B., Santiago, J.V., Malepati, S., Cheng, L., Xiao, H., Duong, D. D., Seyfried, N.T., Wood, L.B., Rowan, M.J.M., Rangaraju, S., 2024. Native-state proteomics of Parvalbumin interneurons identifies unique molecular signatures and vulnerabilities to early Alzheimer's pathology. Nat. Commun. 15, 1–26. https://doi.org/10.1038/s41467-024-47028-7.

- Laham, B.J., Gore, I.R., Brown, C.J., Gould, E., 2024. Adult-born granule cells modulate CA2 network activity during retrieval of developmental memories of the mother. eLife 12, RP90600. https://doi.org/10.7554/elife.90600.
- Lemaire, M., 2003. Social recognition task in the rat. Curr. Protoc. Pharmacol. https://doi.org/10.1002/0471141755.PH0530S20. Chapter 5.
- Li, W., Li, S., Shen, L., Wang, J., Wu, X., Li, J., Tu, C., Ye, X., Ling, S., 2019. Impairment of dendrodendritic inhibition in the olfactory bulb of APP/PS1 mice. Front. Aging Neurosci. 11. https://doi.org/10.3389/FNAGI.2019.00002.
- Livingston, G., Sommerlad, A., Orgeta, V., Costafreda, S.G., Huntley, J., Ames, D., Ballard, C., Banerjee, S., Burns, A., Cohen-Mansfield, J., Cooper, C., Fox, N., Gitlin, L. N., Howard, R., Kales, H.C., Larson, E.B., Ritchie, K., Rockwood, K., Sampson, E.L., Mukadam, N., 2017. Dementia prevention, intervention, and care. The Lancet 390 (10113), 2673–2734. https://doi.org/10.1016/S0140-6736(17)31363-6.
- Locci, A., Orellana, H., Rodriguez, G., Gottliebson, M., McClarty, B., Dominguez, S., Keszycki, R., Dong, H., 2021. Comparison of memory, affective behavior, and neuropathology in APPNLGF knock-in mice to 5xFAD and APP/PS1 mice. Behav. Brain Res. 404. https://doi.org/10.1016/J.BBR.2021.113192.
- Lopez, D.C., White, Z.J., Hall, S.E., 2024. Anxiety in Alzheimer's disease rats is independent of memory and impacted by genotype, age, sex, and exercise. Alzheimers Dement. 20, 3543–3550. https://doi.org/10.1002/ALZ.13813.
- Maaswinkel, H., Baars, A.M., Gispen, W.H., Spruijt, B.M., 1996. Roles of the basolateral amygdala and hippocampus in social recognition in rats. Physiol. Behav. 60, 55–63. https://doi.org/10.1016/0031-9384(95)02233-3.
- Mazzi, C., Massironi, G., Sanchez-Lopez, J., De Togni, L., Savazzi, S., 2020. Face recognition deficits in a patient with Alzheimer's disease: amnesia or agnosia? The importance of electrophysiological markers for differential diagnosis. Front. Aging Neurosci. 12, 580609. https://doi.org/10.3389/FNAGI.2020.580609.
- Misrani, A., Tabassum, Sidra, Huo, Q., Tabassum, Sumaiya, Jiang, J., Ahmed, A., Chen, X., Zhou, J., Zhang, J., Liu, S., Feng, X., Long, C., Yang, L., 2021. Mitochondrial deficits with neural and social damage in early-stage Alzheimer's disease model mice. Front. Aging Neurosci. 13. https://doi.org/10.3389/ FNAGL2021.748388.
- Mitrano, D.A., Houle, S.E., Pearce, P., Quintanilla, R.M., Lockhart, B.K., Genovese, B.C., Schendzielos, R.A., Croushore, E.E., Dymond, E.M., Bogenpohl, J.W., Grau, H.J., Webb, L.S., 2021. Olfactory dysfunction in the 3xTg-AD model of Alzheimer's disease. IBRO Neurosci. Rep. 10, 51–61. https://doi.org/10.1016/J. IBNEUR.2020.12.004.
- Moradi, F., van den Berg, M., Mirjebreili, M., Kosten, L., Verhoye, M., Amiri, M., Keliris, G.A., 2023. Early classification of Alzheimer's disease phenotype based on hippocampal electrophysiology in the TgF344-AD rat model. iScience 26, 107454. https://doi.org/10.1016/J.ISCI.2023.107454.
- Nelis, S.M., Clare, L., Martyr, A., Markova, I., Roth, I., Woods, R.T., Whitaker, C.J., Morris, R.G., 2011. Awareness of social and emotional functioning in people with early-stage dementia and implications for carers. Aging Ment. Health 15, 961–969. https://doi.org/10.1080/13607863.2011.575350.
- Oakley, H., Cole, S.L., Logan, S., Maus, E., Shao, P., Craft, J., Guillozet-Bongaarts, A., Ohno, M., Disterhoft, J., Van Eldik, L., Berry, R., Vassar, R., 2006. Intraneuronal beta-amyloid aggregates, neurodegeneration, and neuron loss in transgenic mice with five familial Alzheimer's disease mutations: potential factors in amyloid plaque formation. J. Neurosci. 26, 10129–10140. https://doi.org/10.1523/JNEUROSCI.1202-06.2006.
- Ognjanovski, N., Schaeffer, S., Wu, J., Mofakham, S., Maruyama, D., Zochowski, M., Aton, S.J., 2017. Parvalbumin-expressing interneurons coordinate hippocampal network dynamics required for memory consolidation. Nat. Commun. 8. https://doi. org/10.1038/NCOMMSI5039
- Park, K., Lee, J., Jang, H.J., Richards, B.A., Kohl, M.M., Kwag, J., 2020. Optogenetic activation of parvalbumin and somatostatin interneurons selectively restores thetanested gamma oscillations and oscillation-induced spike timing-dependent long-term potentiation impaired by amyloid β oligomers. BMC Biol. 18. https://doi.org/10.1186/S12915-019-0732-7.
- Paxinos, G., Watson, C., 2007. The Rat Brain in Stereotaxic Coordinates, 6th ed. Academic Press.
- Pena, R.R., Pereira-Caixeta, A.R., Moraes, M.F.D., Pereira, G.S., 2014. Anisomycin administered in the olfactory bulb and dorsal hippocampus impaired social recognition memory consolidation in different time-points. Brain Res. Bull. 109, 151–157. https://doi.org/10.1016/J.BRAINRESBULL.2014.10.009.
- Pentkowski, N.S., Berkowitz, L.E., Thompson, S.M., Drake, E.N., Olguin, C.R., Clark, B.J., 2018. Anxiety-like behavior as an early endophenotype in the TgF344-AD rat model of Alzheimer's disease. Neurobiol. Aging 61, 169–176. https://doi.org/10.1016/J. NEUROBIOLAGING.2017.09.024.
- Perusini, J.N., Cajigas, S.A., Cohensedgh, O., Lim, S.C., Pavlova, I.P., Donaldson, Z.R., Denny, C.A., 2017. Optogenetic stimulation of dentate gyrus engrams restores memory in Alzheimer's disease mice. Hippocampus 27, 1110–1122. https://doi.org/ 10.1002/HIPO.22756
- Petrasek, T., Vojtechova, I., Lobellova, V., Popelikova, A., Janikova, M., Brozka, H., Houdek, P., Sladek, M., Sumova, A., Kristofikova, Z., Vales, K., Stuchlík, A., 2018. The McGill transgenic rat model of Alzheimer's disease displays cognitive and motor impairments, changes in anxiety and social behavior, and altered circadian activity. Front. Aging Neurosci. 10, 250. https://doi.org/10.3389/FNAGI.2018.00250/ RIRTEX
- Pietropaolo, S., Delage, P., Lebreton, F., Crusio, W.E., Cho, Y.H., 2012. Early development of social deficits in APP and APP-PS1 mice. Neurobiol. Aging 33, 1002. e17–1002.e27. https://doi.org/10.1016/J.NEUROBIOLAGING.2011.09.012.
- Piskorowski, R.A., Chevaleyre, V., 2013. Delta-opioid receptors mediate unique plasticity onto parvalbumin-expressing interneurons in area CA2 of the hippocampus. J. Neurosci. 33, 14567. https://doi.org/10.1523/JNEUROSCI.0649-13.2013.

- Poon, C.H., Wong, S.T.N., Roy, J., Wang, Y., Chan, H.W.H., Steinbusch, H., Blokland, A., Temel, Y., Aquili, L., Lim, L.W., 2023. Sex differences between neuronal loss and the early onset of amyloid deposits and behavioral consequences in 5xFAD transgenic mouse as a model for Alzheimer's disease. Cells 12. https://doi.org/10.3390/ CFLIS12050780
- Rey, C.C., Robert, V., Bouisset, G., Loisy, M., Lopez, S., Cattaud, V., Lejards, C., Piskorowski, R.A., Rampon, C., Chevaleyre, V., Verret, L., 2022. Altered inhibitory function in hippocampal CA2 contributes in social memory deficits in Alzheimer's mouse model. iScience 25. https://doi.org/10.1016/J.ISCI.2022.103895.
- Roberts, R.O., Christianson, T.J.H., Kremers, W.K., Mielke, M.M., Machulda, M.M., Vassilaki, M., Alhurani, R.E., Geda, Y.E., Knopman, D.S., Petersen, R.C., 2016. Association between olfactory dysfunction and amnestic mild cognitive impairment and Alzheimer disease dementia. JAMA Neurol. 73, 93. https://doi.org/10.1001/ JAMANEUROL.2015.2952.
- Rorabaugh, J.M., Chalermpalanupap, T., Botz-Zapp, C.A., Fu, V.M., Lembeck, N.A., Cohen, R.M., Weinshenker, D., 2017. Chemogenetic locus coeruleus activation restores reversal learning in a rat model of Alzheimer's disease. Brain 140 (11), 3023–3038. https://doi.org/10.1093/brain/awx232.
- Ruden, J.B., Dugan, L.L., Konradi, C., 2021. Parvalbumin interneuron vulnerability and brain disorders. Neuropsychopharmacology: Official Publication of the American College of Neuropsychopharmacology 46 (2), 279–287. https://doi.org/10.1038/ \$41386-020-0778-9.
- Saré, R.M., Cooke, S.K., Krych, L., Zerfas, P.M., Cohen, R.M., Smith, C.B., 2020. Behavioral phenotype in the TgF344-AD rat model of Alzheimer's disease. Front. Neurosci. 14. https://doi.org/10.3389/FNINS.2020.00601/FULL.
- Savaskan, E., Summermatter, D., Schroeder, C., Schächinger, H., 2018. Memory deficits for facial identity in patients with amnestic mild cognitive impairment (MCI). PLoS One 13, e0195693. https://doi.org/10.1371/JOURNAL.PONE.0195693.
- Schweinfurth, M.K., 2020. The social life of Norway rats (Rattus norvegicus). ELife 9. https://doi.org/10.7554/ELIFE.54020.
- Semple-Rowland, S.L., Dawson, W.W., 1987. Cyclic light intensity threshold for retinal damage in albino rats raised under 6 Lx. Exp. Eye Res. 44, 643–661. https://doi.org/ 10.1016/S0014-4835(87)80136-7.
- Shih, Y.T., Alipio, J.B., Sahay, A., 2023. An inhibitory circuit-based enhancer of DYRK1A function reverses Dyrk1a-associated impairment in social recognition. Neuron 111. https://doi.org/10.1016/J.NEURON.2023.09.009, 3084-3101.e5.
- Smith, L.A., McMahon, L.L., 2018. Deficits in synaptic function occur at medial perforant path-dentate granule cell synapses prior to Schaffer collateral-CA1 pyramidal cell synapses in the novel TgF344-Alzheimer's disease rat model. Neurobiol. Dis. 110, 166–179. https://doi.org/10.1016/j.nbd.2017.11.014.
- Song, Z., Swarna, S., Manns, J.R., 2021. Prioritization of social information by the basolateral amygdala in rats. Neurobiol. Learn. Mem. 184, 107489. https://doi.org/ 10.1016/J.NLM.2021.107489.
- Srivastava, H., Lasher, A.T., Nagarajan, A., Sun, L.Y., 2023. Sexual dimorphism in the peripheral metabolic homeostasis and behavior in the TgF344-AD rat model of Alzheimer's disease. Aging Cell 22, e13854. https://doi.org/10.1111/ACEL.13854.
- Stackman, R.W., Cohen, S.J., Lora, J.C., Rios, L.M., 2016. Temporary inactivation reveals that the CA1 region of the mouse dorsal hippocampus plays an equivalent role in the retrieval of long-term object memory and spatial memory. Neurobiol. Learn. Mem. 133. 118–128. https://doi.org/10.1016/J.NI.M.2016.06.016.
- Stevenson, E.L., Caldwell, H.K., 2014. Lesions to the CA2 region of the hippocampus impair social memory in mice. Eur. J. Neurosci. 40, 3294–3301. https://doi.org/ 10.1111/F.IN.12689
- Stoiljkovic, M., Kelley, C., Stutz, B., Horvath, T.L., Hajós, M., 2019. Altered cortical and hippocampal excitability in TgF344-AD rats modeling Alzheimer's disease pathology. Cereb. Cortex 29, 2716–2727. https://doi.org/10.1093/CERCOR/ BHY140.
- Sun, Y., 2023. Investigating Associations Between Electrophysiological and Pathological Changes in the TgF344-AD Rat Model for Alzheimer's Disease. Doctoral dissertation. The University of Manchester. https://pure.manchester.ac.uk/ws/portalfiles/por tal/272870534/FULL TEXT.PDF.
- Tatsukawa, T., Ogiwara, I., Mazaki, E., Shimohata, A., Yamakawa, K., 2018. Impairments in social novelty recognition and spatial memory in mice with conditional deletion of Scn1a in parvalbumin-expressing cells. Neurobiol. Dis. 112, 24–34. https://doi.org/ 10.1016/J.NBD.2018.01.009.
- Terstege, D.J., Epp, J.R., 2023. Parvalbumin as a sex-specific target in Alzheimer's disease research – a mini-review. Neurosci. Biobehav. Rev. 153, 105370. https://doi. org/10.1016/j.neubiorev.2023.105370.
- Thor, D.H., Holloway, W.R., 1982. Social memory of the male laboratory rat. J. Comp. Physiol. Psychol. 96, 1000–1006. https://doi.org/10.1037/0735-7036.96.6.1000.
- Tort, A.B.L., Kramer, M.A., Thorn, C., Gibson, D.J., Kubota, Y., Graybiel, A.M., Kopell, N. J., 2008. Dynamic cross-frequency couplings of local field potential oscillations in rat striatum and hippocampus during performance of a T-maze task. Proc. Natl. Acad. Sci. USA 105, 20517–20522. https://doi.org/10.1073/PNAS.0810524105.
- Tort, A.B.L., Komorowski, R.W., Manns, J.R., Kopell, N.J., Eichenbaum, H., 2009. Theta-gamma coupling increases during the learning of item-context associations. Proc. Natl. Acad. Sci. USA 106, 20942–20947. https://doi.org/10.1073/ DNAS.0011321106
- Tournier, B.B., Barca, C., Fall, A.B., Gloria, Y., Meyer, L., Ceyzériat, K., Millet, P., 2021. Spatial reference learning deficits in absence of dysfunctional working memory in the TgF344-AD rat model of Alzheimer's disease. Genes Brain Behav. 20, e12712. https://doi.org/10.1111/GBB.12712.
- Toyoshima, M., Yamada, K., 2023. Enhanced social motivation in briefly isolated male rats. IBRO Neurosci. Rep. 15, 203–208. https://doi.org/10.1016/J. IBNEUR.2023.08.2195.

- van den Berg, M., Toen, D., Verhoye, M., Keliris, G.A., 2023. Alterations in theta-gamma coupling and sharp wave-ripple, signs of prodromal hippocampal network impairment in the TgF344-AD rat model. Frontiers in Aging Neuroscience 15, 1081058. https://doi.org/10.3389/FNAGI.2023.1081058/BIBTEX.
- Várkonyi, D., Török, B., Sipos, E., Fazekas, C.L., Bánrévi, K., Correia, P., Chaves, T., Farkas, S., Szabó, A., Martínez-Bellver, S., Hangya, B., Zelena, D., 2022. Investigation of anxiety- and depressive-like symptoms in 4- and 8-month-old male triple transgenic mouse models of Alzheimer's disease. Int. J. Mol. Sci. 23. https://doi.org/10.3390/IJMS231810816.
- Xia, F., Richards, B.A., Tran, M.M., Josselyn, S.A., Takehara-Nishiuchi, K., Frankland, P. W., 2017. Parvalbumin-positive interneurons mediate neocortical-hippocampal
- interactions that are necessary for memory consolidation. Elife 6. https://doi.org/ 10.7554/ELIFE.27868.
- Yang, J.T., Wang, Z.J., Cai, H.Y., Yuan, L., Hu, M.M., Wu, M.N., Qi, J.S., 2018. Sex differences in neuropathology and cognitive behavior in APP/PS1/tau tripletransgenic mouse model of Alzheimer's disease. Neurosci. Bull. 34, 736. https://doi. org/10.1007/S12264-018-0268-9.
- Zhang, Haiwang, Ben Zablah, Y., Liu, A., Lee, D., Zhang, Haorui, Meng, Y., Zhou, C., Liu, X., Wang, Y., Jia, Z., 2021. Overexpression of LIMK1 in hippocampal excitatory neurons improves synaptic plasticity and social recognition memory in APP/PS1 mice. Mol. Brain 14. https://doi.org/10.1186/S13041-021-00833-3.